# Master's Thesis

# The Inverse Problem of Photothermal Measurement of Layer Thicknesses in Multilayered Systems

Faculty of Mathematics and Computer Science
Department of Mathematics
Saarland University

## Eileen Oberringer

Saarbrücken, June, 2022

Submitted in partial fulfillment of the requirements for the degree of M. Sc.

Supervisor:            Prof. Dr. Thomas Schuster

Advisor:               Dr. Dimitri Rothermel

First Reviewer:        Prof. Dr. Thomas Schuster

Second Reviewer:       Prof. Dr. Sergej Rjasanow

Submission Date:       June 22, 2022


Name:                  Eileen Oberringer

Matriculation Number:  2563114

E-Mail:                oberringereileen@gmail.com

Address:               Försterstraße 70 F309

                       66111 Saarbrücken

# Declaration of Authorship

I hereby declare that the report submitted is my own unaided work. All direct or indirect sources used are acknowledged as references. I am aware that the Thesis in digital form can be examined for the use of unauthorized aid and in order to determine whether the report as a whole or parts incorporated in it may be deemed as plagiarism. For the comparison of my work with existing sources I agree that it shall be entered in a database where it shall also remain after examination, to enable comparison with future Theses submitted. Further rights of reproduction and usage, however, are not granted here. This paper was not previously presented to another examination board and has not been published.

Saarbrücken, June 22, 2022

_____

Name

# Abstract

Nondestructive testing and evaluation summarizes numerous techniques that aim to test and evaluate the properties of materials without causing damage. Particularly, utilizing photothermal science, which is based on the observation that optical energy (light) is absorbed by media and converted into thermal energy (heat), is promising when it comes to that goal. First steps in this field were already taken in the mid 1970s by introducing *photoacoustic spectroscopy*. This approach to detect material's properties further exploits the fact that a periodical modulation of said optical energy leads to an audible sound. In today's applications, the previously described *photothermal effect* is primarily used to generate a modulated heating. The resulting temperature changes are then directly analyzed to provide certain properties as well as defects of the considered object.

In this thesis, we specialize in the *photothermal measurement of layer thicknesses in multilayered systems* as an application by observing and understanding the problem in the context of inverse problems. In particular, we focus on the introduction of the mathematical model of said inverse problem. Furthermore, we utilize this conception to run a minor study providing an overview of some photothermal measurement experiments. The results of said study confirm the applicability of photothermal science for the mentioned use, as well as verify some theoretical findings.

# Danksagung

An dieser Stelle möchte ich mich bei allen Personen, die mich während meines Studiums und insbesondere während des Schreibprozesses dieser Masterarbeit unterstützt haben, bedanken.

Zuallererst möchte ich mich sowohl bei meiner Familie als auch bei meinen Freunden für die große Unterstützung in den letzten Jahren bedanken. Ein besonderer Dank gilt dabei Kevin Müller, sowohl für das wiederholte Korrekturlesen, als auch allgemein für die riesige Unterstützung jeglicher Art.

Weiter danke ich Herrn Prof. Dr. Thomas Schuster, sowohl für die Möglichkeit aktiv in der aktuellen Forschung zur zerstörungsfreien Prüfung, welche zu dem Thema meiner Masterarbeit geführt hat, mitzuarbeiten, als auch für die gute Betreuung. Außerdem danke ich Herrn Prof. Dr. Sergey Rjasanow für die Zweitkorrektur dieser Arbeit.

Besonders möchte ich Herrn Dr. Dimitri Rothermel für die hilfreichen Gespräche, die mir immer dann die nötigen Denkanstöße gaben, wenn ich nicht mehr weiter wusste, als auch für das Korrekturlesen danken.

# Contents

# Symbols and abbreviations

| | |
|---|---|
| $A_0$ | Thermal wave amplitude at point of generation |
| $\alpha$ | Thermal diffusivity |
| $\beta$ | Optical absorption coefficient |
| $C$ | Heat capacity |
| $c$ | Specific heat capacity |
| $e$ | Effusivity |
| $\varepsilon$ | Emissivity |
| $f$ | Frequency |
| $\varphi$ | Thermal wave phase angle |
| $\Gamma$ | Effective thermal wave reflection coefficient |
| $I$ | Optical intensity |
| Im | Imaginary part of |
| $\kappa$ | Thermal conductivity |
| $L$ | Layer thickness |
| $\lambda$ | Wavelength |
| $M$ | Material |
| $\rho$ | Density |
| $\rho c$ | Volumetric specific heat |
| $Q$ | Heat pulse energy |
| $Q_0$ | Heat source intensity |
| $q$ | Heat flux |
| $R$ | Interface thermal wave reflection coefficient |
| Re | Real part of |
| $\sigma$ | Thermal wave number |
| $\sigma_{\mathrm{SB}}$ | Stefan Boltzmann constant |
| $T$ | Thermal wave transmission coefficient |
| $\tilde{T}$ | Temperature amplitude |
| $T(x,t)$ | Periodic temperature, dependent on position and time |
| $\mu$ | Thermal diffusion length |
| $\omega$ | Modulation frequency |

# 1 Introduction

## 1.1 General Motivation

Based on the physical observation that optical energy (light) is absorbed and converted into thermal energy (heat), the field of photothermal science is born. The area includes a broad and manifold range of techniques used, amongst others, in the constantly growing field of nondestructive testing and evaluation. It is assumed that the previously described observation which we call the *photothermal effect* was firstly discovered by *Jean Joseph Baptiste Fourier*, already in the beginning of the 19th century, by investigating at which depth certain water pipelines freeze in winter. His research resulted in his famous work "Théorie analytique de la chaleur" (see [1]) with which he laid the foundations of today's knowledge of heat transfer. Building on this knowledge, many other scientists refined his work, resulting in many different fields of application.

In this thesis, we join the theory of photothermal science with the mathematical field of inverse problems, resulting in the inverse problem of *photothermal measurement of layer thicknesses in multilayered systems*. Said systems are mainly built according to the subsequent figure:
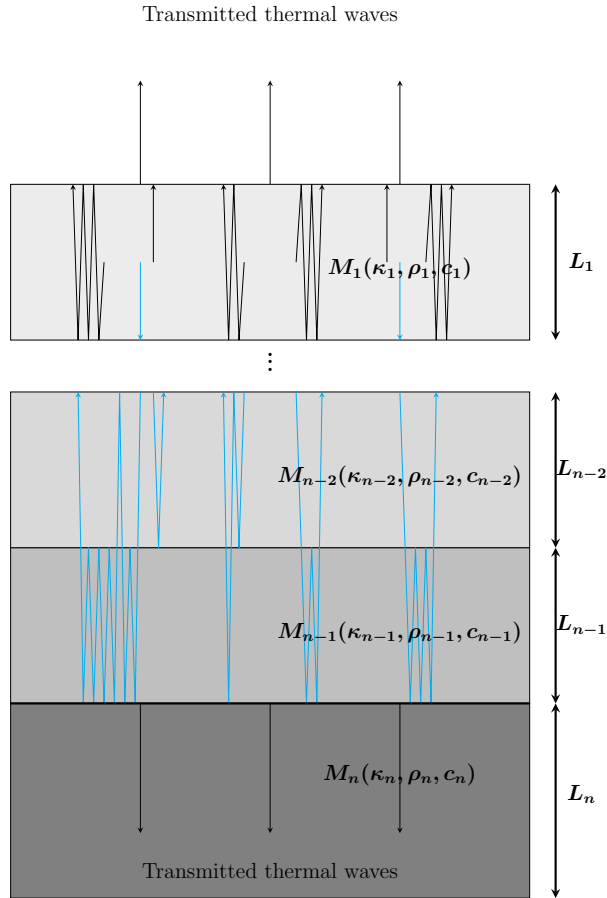


Figure 1: System of $n-1$ layers of coating $M_1$ - $M_{n-1}$ and one layer of substrate $M_n$

Here, $M_1$ - $M_{n-1}$ are different coating layers and $M_n$ is a (metallic) substrate layer. The goal is to determine the layer thicknesses of the coating layers $M_1$ - $M_{n-1}$, i.e., interior properties that are not directly accessible, by processing exterior data in the form of the measured surface temperature of such a system. Thus, the problem is very suitable to be understood in terms of inverse problems.

Before being able to do so, we need to establish some crucial facts. Thus, in the current section, we are further equipped with a brief and quick introduction into the field of *infrared thermography*, providing a classification of *infrared light* as well as an explanation of the measurement principle in *infrared thermography*. We distinguish between two different excitation modes, namely *pulse* and *lock-in thermography*, before we limit ourselves to the latter, which consists in a planar, sinusoidal excitation of the surface of the system. In this context, we define the thermal diffusion length:

$$\mu = \sqrt{\frac{2\alpha}{\omega}}$$

depending on the material's *thermophysical properties* as well as the specific *excitation frequency* $\omega$. It determines the depth reach of the thermal waves into the material and thus the adequate area in the measurement process.

Subsequently, we provide the complete physical and mathematical background of photothermal science. In a first step, we take a closer look at the composition of media, resulting in the definition of the *thermophysical properties* of media, characterizing their behavior when it comes to heating and cooling effects. Via these fundamentals, we investigate *heat transfer*, leading to the introduction of the term *thermal wave* as well as their *reflection* and *refraction* effects. A *thermal wave* is mathematically spoken no more than a solution of a certain partial differential equation, namely the *heat diffusion equation*, to whose derivation we further pay great attention.

The third section represents the heart of this thesis: Thanks to the aforementioned observations, we are finally able to determine the (complex valued) surface temperature of the previously described multilayered systems, reading:

$$T(x = 0, t) = \tilde{T}(x = 0) \exp\left[i\left(\omega t - \frac{\pi}{4}\right)\right]$$

for a complex term $\tilde{T}(x = 0)$ that is dependent on the material's properties as well as the type of excitation. From this complex quantity we extract its phase angle, possessing the following form:

$$\varphi_{\tilde{T}} = \tan^{-1}\left[\frac{\mathrm{Im}\left[\tilde{T}(x = 0)\right]}{\mathrm{Re}\left[\tilde{T}(x = 0)\right]}\right].$$

This step brings the advantage that the phase angle is a real and measurable quantity leading to the exterior (measured) data that is crucial to define the forward operators.

Those operators take the following form:

$$F_n \colon \left(\mathbb{R}^+\right)^{n+1} \times \mathbb{R}^m \to \mathbb{R}^m,$$

$$F_n(L_1, \ldots, L_{n+1}; \omega_1, \ldots, \omega_m) := \overline{\varphi_{\tilde{T}}}$$

characterizing a system of $n + 2$ layers.

Building on said results, we are finally able to introduce the inverse problem of *photothermal measurement of layer thicknesses in multilayered systems* by performing a nonlinear least squares approach of the following function:

$$F_n(L_1, \ldots, L_{n+1}; \omega_1, \ldots, \omega_m) - \overline{\varphi_{\tilde{T}_{meas}}}.$$

Thus leading to the subsequent inverse operators:

$$G_n \colon \mathbb{R}^m \to \left(\mathbb{R}^+\right)^{n+1},$$

$$G_n(\overline{\varphi_{\tilde{T}_{meas}}}) := \underset{(L_1, \ldots, L_{n+1}) \in (\mathbb{R}^+)^{n+1}}{\arg\min} ||F_n(L_1, \ldots, L_{n+1}; \omega_1, \ldots, \omega_m) - \overline{\varphi_{\tilde{T}_{meas}}}||_2^2.$$

The penultimate section further concerns a brief practical application of said theory by performing some calculation experiments. Via these experiments, we present a short study by testing and validating the algorithm, we programmed according to the mathematical basics introduced in the previous sections by varying the included parameters. We find that the algorithm provides satisfying results when equipped with sufficient data.

Last but not least, the fifth section presents an overview of the obtained results as well as an outlook to problems and opportunities that came or could possibly come up when dealing with real life applications.

## 1.2   Infrared Thermography

Let us turn our attention to the applications of photothermal science. It turns out that photothermal science can be used in the field of non-destructive testing and evaluation. Mainly, there are two major application areas in that field, namely *photoacoustic spectroscopy* as well as *photothermal radiometry*, each of which has several specific application purposes. All these applications are mainly based on the fact that optical energy, i.e., light, is absorbed by media and converted into thermal energy, i.e., heat. In *photoacoustic spectroscopy*, additional use is made of the fact that the targeted modulation of light produces tones that can be perceived by sensitive microphones. Alexander Graham Bell and Charles Sumner Tainter already used this observation for their *photophone* in 1880, which represents a wireless light telephone for the long-distance transmission of sound. In this thesis, however, we specialize in the second application mentioned, namely *photothermal radiometry*. We restrict ourselves to light in the (near) infrared range for both excitation and detection. This method is therefore called *infrared thermography* and counts as *optical thermography* method. In this thesis, we explain both why it is useful to make this limitation and, in general, the advantages of optical thermography methods. Subsequently, we describe the structure of the measurement process, as well as explain the functions of the required devices.

### 1.2.1   Infrared Radiation

We briefly take a closer look at the *electromagnetic spectrum*. We are particularly interested in wavelengths between 0.74 and 1000 micrometers, defining *infrared radiation*. We mainly refer to [2].

All matter emits electromagnetic radiation at all time. The totality of all these types of radiation, which differ in their wavelengths, is called the *electromagnetic spectrum* or *electromagnetic wave spectrum*. The following figure represents the electromagnetic spectrum. In particular, the part of the light that is visible to humans, also called the *light spectrum*:
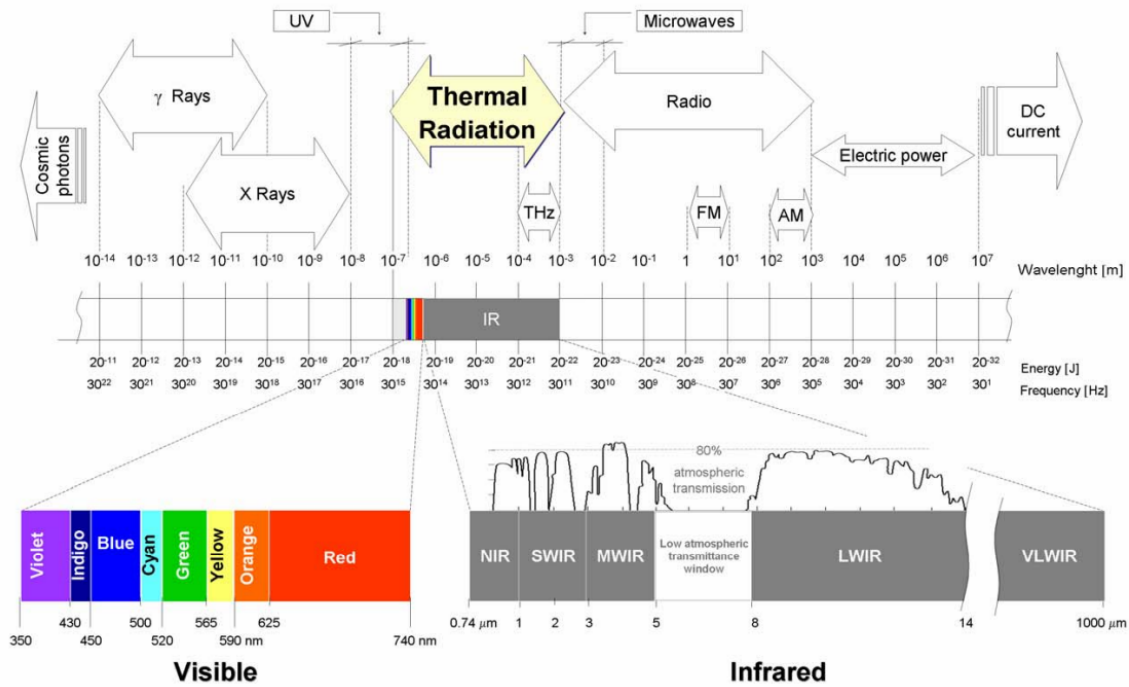
Figure 2: The electromagnetic spectrum, see [2, p. 128]
.

As can be observed in Figure 2, the infrared radiation, which is in the range of *thermal radiation*, is located between the light visible to humans and the terahertz radiation. This range has wavelengths between 0.74 and 1000 micrometers, and frequencies between about 300 gigahertz and 400 terahertz. Furthermore, the infrared spectrum can be further divided into the following categories:

1  near infrared (NIR), $0.74 - 1$ micrometers

2  short wavelength (SWIR), $1 - 3$ micrometers

3  mid-wavelength (MWIR), $3 - 5$ micrometers

4  long-wavelength (LWIR), $8 - 14$ micrometers

5  very long wavelength infrared (VLWIR), $14 - 1000$ micrometers

The measurements are often limited to the near infrared range. This brings a big advantage, because it is directly adjacent to the visible light (it starts directly behind the red light), which is why there is no major danger, compared to for example X-rays or other types of radiation. This means that no major safety precautions need to be taken.

### 1.2.2 Measurement Principle and Setup

Here, we want to introduce the principles of (infrared) thermography as well as the setup of a typical infrared measurement system with all its devices and functions. However, we do not go into much detail about the individual devices. We mainly refer to [2] which can also be used to study additional information on the subject.

Consider the following setup:
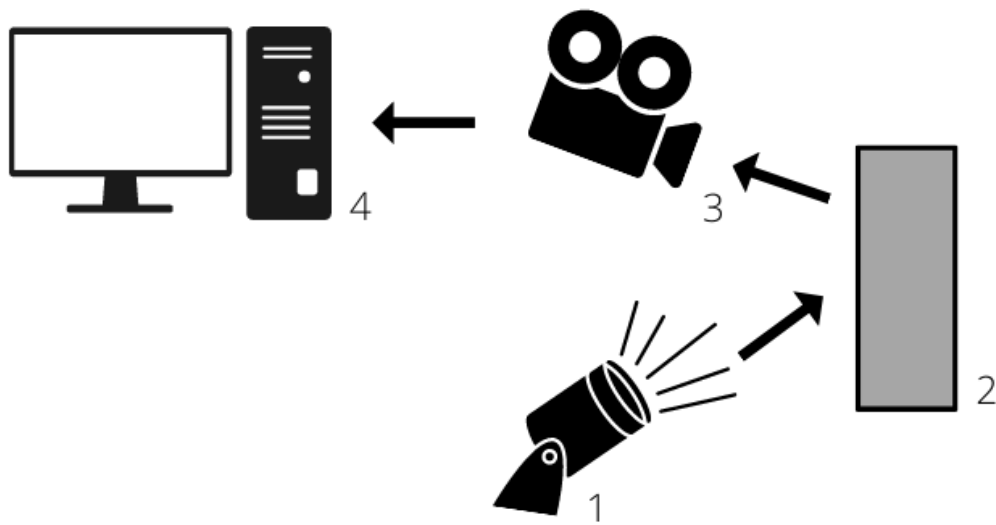


Figure 3: Measurement principle of (infrared) thermography

where component:

1 is a *thermal source of excitation*:
   Its task is to create a thermal gradient between the considered specimen and the environment, so that thermal conduction is established. Therefore, we call this setup *active thermography*. If a thermal contrast between the test object and the environment already exists from the beginning, this excitation is not required, and we speak of *passive thermography*.

2 is the *test object*:
   The measurements are performed on this object. In our case, this is a system of layers consisting of a substrate layer and one or multiple coating layers.

3 is a *measuring device*, also called a *radiometer*:
   In our case, this is an infrared camera that measures the heat on the surface of the test object.

4 is a *device for evaluation/computer*:
   Here the data is then evaluated and processed.

Notice that in each component of this measurement system there arises heat noise, which adds up to a large quantity in the end. For this reason, following the measurement, the last step of signal processing is necessary to reduce noise. This is a very general setup. Of course, we need to specify some components of it more precisely, depending on the type of excitation. Subsequently, we will give a brief introduction to the two most common types of excitation.

### 1.2.3  Types of Excitation

We briefly give a short overview of the two basic excitation types characterizing the thermography method, namely *lock-in excitation* that characterizes *lock-in thermography* and *pulse excitation* characterizing *pulse thermography*, and name their advantages as well as their disadvantages. Although only the latter is relevant for us, we will also introduce the *pulse thermography* since it is easier to compare the advantages and disadvantages of *lock-in thermography* with this method. We will not go into much detail here. We mainly refer to [2, 3, 4, 5, 6, 7, 8] which can also be considered for more information.

**Pulse Thermography**

In pulse thermography, the test object is excited by a high energy heat pulse, in general in the form of a set of flashlights or a laser, in a short period of time to heat the objects surface. The time period in this process varies from a few milliseconds to a few seconds, depending on the sample's thermal properties. In the meantime, the temperature profile on the surface of the specimen is acquired by a thermal camera and subsequently processed.

Pulse thermography comes with some advantages, namely:

(1) Since the excitation is done with a pulse, that is mathematically a sum of many different excitation frequencies, we get a large amount of data about different frequencies and thus different depths of the object. Consequently, we already obtain a great deal of information about the test object in a single test.

(2) The process is very fast, usually only a few milliseconds to seconds are sufficient to collect enough information.

Unfortunately, the method has its disadvantages, namely:

(1) In order to obtain all the information that is theoretically possible in one experiment, high requirement of the thermal equipment in form of a thermal camera with a high frame rate to capture all the information in this short period of time is needed.

(2) A high amount of energy is needed to generate the pulse.

(3) Non-uniform heating has a very strong influence on the measurement results. This in turn results in a higher requirement of the thermal imaging equipment, as well as more frequent post-processing to reduce noise.

**Lock-in Thermography**

In lock-in thermography, the test object is heated by an external modulated periodic excitation (of a single specific excitation frequency), from which thermal waves are generated near the surface. In general, this is done by optical radiation in the form of lasers or halogen lamps. At the same time, the surface temperature of the test object is measured and analyzed by a thermal camera. Subsequently, by making use of the excitation frequency and phase, in the post-process, a *lock-in amplifier* is used to determine the phase and amplitude lag of the noisy signal from the recorded temperature profile at the surface in reference to the modulation signal. In principle, this step can be seen as a small bandwidth filtering resulting in two dc voltages. For more information about the functionality of a lock-in amplifier, see [8, 9]. In the process, the depth range can be determined by the *thermal diffusion length*:

$$\mu = \sqrt{\frac{2\alpha}{\omega}},$$

where $\alpha$ denotes the thermal diffusivity and $\omega := 2\pi f$ denotes the excitation frequency. In the process of the photothermal measurement of layer thicknesses, these phase images are then used after the measurement to assign the correct layer thicknesses of the object.

The method has some great advantages, namely:

(1) Since we only excite with a certain frequency, we only have to deal with a low requirement on the intensity of the excitation.

(2) Also, due to the specific excitation frequency, we can precisely control the depth range. This is especially helpful when it comes to defect characterization, and we know approximately at which depth the defect is located.

(3) Signal processing is a very simple process, as the phase images can be quickly and easily calculated from the temperature profiles.

(4) The calculated phase information is not very sensitive to external influences, such as reflections from the environment, surface emissivity variations and non-uniform heating, which means that we obtain a good signal-to-noise ratio.

(5) The measurement result is not influenced by non-uniform excitation.

(6) The method can be well adapted to curved surfaces.

However, this method also has disadvantages, namely:

(1) Since the depth range is determined by the thermal diffusion length, which depends on the frequency, we examine only one specific thickness per experiment. This means that we would usually have to make several experiments with different excitation frequencies in order to investigate the entire thickness of the layer. However, this is rather important when investigating defects, which we do not discuss further in this thesis.

(2) The experimental setup is not quite simple, since we need additional devices, such as a lock-in amplifier.

(3) The measurement takes a relatively long time, as we perform it for at least one entire excitation cycle.

Following these brief introductions to the two most prominent types of thermography, it can be stated overall that the advantages of one method are more or less the disadvantages of the other, and vice versa. It is therefore obvious to combine these two methods. This is done, for example, in *pulse-phase thermography* which roughly speaking uses the pulse excitation to then proceed with the help of Fourier transformation as in the lock-in thermography, i.e., phase analysis in frequency domain of the pulse thermography. However, we will not go into this further. For more information, see [2] or [3].

We limit ourselves to lock-in thermography because of the simplicity and sufficient potency of the method for our purposes. However, pulse thermography would generally be better suited for defect characterization. Subsequently, we summarize both the advantages and the disadvantages of those two methods. It should be mentioned that, of course, the major advantage both of these methods offer is the contactless and nondestructive measurement principle.

| Advantages and disadvantages of both methods | | |
|---|---|---|
| | Advantages | Disadvantages |
| Pulse Thermography | High information coverage in a single application | High energy requirement |
| | Fast | High camera frame rate |
| | | High impairment by non-uniform heating |
| | | Expensive equipement |
| Lock-in thermography | Simple signal processing | Dependency of $\mu$ on excitation frequency $\omega$ |
| | Low energy waves | Complex configuration |
| | Non-impairment by non-uniform heating | Slow |
| | Simple variation of depth reach | |
| | High signal-to-noise ratio | |
| | Good adaptability to curvature surface | |

Table 1: Advantages and disadvantages of pulsed thermography and lock-in thermography, see [2, p. 25]

In the further course, we specify in an excitation with one certain frequency, corresponding to lock-in thermography and derive the mathematical foundations for that setting.

# 2   Physical and Mathematical Background

This section serves as an introduction to the main physical and mathematical principles of photothermal science. More specifically, the *thermophysical properties* of materials are introduced and discussed. This is followed by an introduction to the three *types of heat transfer*. In particular, we look at *heat conduction* and derive the *heat diffusion equation* along with solutions that define the term *thermal wave*. Consequently, we give a short overview of reflection and refraction effects, which occur similarly to acoustic waves.

## 2.1   Thermophysical Properties of Materials

In this subsection, we discuss the *thermophysical properties* that each material possesses. In particular, we consider the *density*, the *thermal conductivity* as well as the *specific heat capacity*. All these properties precisely characterize the material and influence the heat flow that occurs in it. We mainly refer to [10, 11].

*Density*
The density of a material (also known as *volumetric mass density* or *specific mass*) is defined as the mass per unit volume, more precisely the quotient of the mass of the material and its volume. We denote it by $\rho$. Its SI unit is given by $\frac{\text{kg}}{\text{m}^3}$.

*Heat capacity*
The *heat capacity* of a material is defined as the quantity of heat required to increase its entire temperature by a unit. We denote it by $C$. Its SI unit is given by $\frac{\text{J}}{\text{K}}$.

*Specific heat capacity*
The *specific heat capacity* of a material is defined as the quantity of heat required to increase a unit mass of the material by a unit, i.e., the ratio of the material's heat capacity and its mass. We denote it by $c$. Its SI unit is given by $\frac{\text{J}}{\text{kgK}}$.

*Thermal conductivity*
The *thermal conductivity* of a substance is defined as the quantity of heat passing per unit time normally through unit area of a material of unit thickness for unit temperature difference between the faces, i.e., it describes the materials' ability to conduct heat. We denote it by $\kappa$. Its SI unit is given by $\frac{\text{W}}{\text{mK}}$.

In this thesis, we often need a single expression that takes all of these three properties into account. For that reason, we firstly define the *thermal diffusivity* by:

$$\alpha := \frac{\kappa}{\rho c}. \tag{2.1}$$

Notice that we denote the product $\rho c$ as *volumetric specific heat*. Roughly speaking, thermal diffusivity indicates the temperature's distribution in a medium in non-steady

state, i.e., when the medium is heated or cooled down. Consequently, it is a measure of the ease with which heat is carried through the material by conduction. The thermal diffusivity plays a significant role in the heat diffusion equation, as becomes clear in the next subsection. Its SI unit is given by $\frac{\text{m}^2}{\text{s}}$. Secondly, we further define the *thermal effusivity* by

$$\boldsymbol{e} \coloneqq \sqrt{\kappa \rho c}. \tag{2.2}$$

Roughly speaking, the thermal effusivity of a material is a measure of how "well" thermal energy is exchanged with the material's surroundings. Its SI unit is given by $\frac{\text{J}}{\text{m}^2\text{K}\sqrt{\text{s}}}$.

Note that materials possessing high diffusivities generally also possess high effusivities. Nevertheless, there are also some exceptions. The best known example is air, which has a high diffusivity due to its very low thermal conductivity and density, but a low effusivity. In non-destructive testing, we exploit this property. Depending on the context, we use either the thermal diffusivity or the thermal effusivity.

In the following, we give a small table containing the thermophysical properties of some materials, divided into metals and non-metals. Note that most metals generally have a higher thermal conductivity than most non-metals, whereas most non-metals have a higher specific heat capacity than most metals. Subsequently, in the *photothermal measurement of layer thicknesses in multilayered systems*, we generally consider systems consisting of a substrate layer, which is usually made of a metal, and one, or more different coating layers possessing different thermophysical properties. This provides us with a contrast between said properties of the individual materials at each interface, allowing us to distinguish the materials in the measurement process.

| Some common materials and their thermophysical properties | | | |
|---|---|---|---|
| Material | Density $\left[\frac{\text{kg}}{\text{m}^3}\right]$ | Specific heat capacity $\left[\frac{\text{J}}{\text{kgK}}\right]$ | Thermal conductivity $\left[\frac{\text{W}}{\text{mK}}\right]$ |
| Metals | | | |
| Pure aluminium | 2700 | 945 | 238 |
| Al alloy 2024-T6 | 2770 | 875 | 177 |
| Chromium | 7160 | 449 | 93.7 |
| Pure cooper | 8933 | 385 | 401 |
| Bronze 90 Gold | 19300 | 129 | 317 |
| Pure iron | 7870 | 447 | 80.2 |
| Steel AISI 1010 | 7832 | 434 | 63.9 |
| Steel AISI 316 | 8238 | 468 | 13.4 |
| Lead | 11340 | 129 | 35.3 |
| Magnesium | 1740 | 1024 | 156 |
| Molybdenum | 10240 | 251 | 138 |
| Pure nickel | 8900 | 444 | 138 |
| Inconel X-750 | 8510 | 439 | 11.7 |
| Silver | 10500 | 235 | 429 |
| Titanium | 4500 | 522 | 21.9 |
| Tungsten | 19300 | 132 | 174 |
| Zinc | 7140 | 389 | 116 |
| Zirconium | 6570 | 278 | 22.7 |
| Non-metals | | | |
| Aluminium oxide | 3970 | 765 | 46 |
| Beryllium oxide | 3000 | 1030 | 272 |
| Diamond IIa | 3500 | 509 | 2300 |
| Silicon carbide | 3160 | 675 | 490 |
| Silicon nitride | 2400 | 691 | 16 |
| Germanium | 5360 | 322 | 59.9 |
| Silicon | 2330 | 712 | 148 |
| Quartz glass | 2210 | 730 | 1.4 |
| Bakelite | 1270 | 1590 | 0.23 |
| Rubber (soft) | 1100 | 2010 | 0.13 |
| Wood (oak) | 545 | 2385 | 0.17 |
| Lubrication oil | 845 | 2020 | 0.14 |
| Air | 1.16 | 1007 | 0.026 |

Table 2: Thermophysical properties of some common materials, divided into metals and non-metals, see [12, p. 16-17]

## 2.2 Heat Transfer and the Heat Diffusion Equation

This subsection focuses on heat transfer in materials. In this regard, we define and explain the *three types of heat transfer* that occur in media. We specialize in *heat conduction*, which is mathematically characterised by the *heat diffusion equation*. Furthermore, we solve the aforementioned equation in one certain case. Based on this process, we introduce the concept of *thermal waves* as well as their generation. This is done quite analogously to the case of electromagnetic and acoustic waves. We mainly refer to [12, 13].

### 2.2.1 Heat Transfer Modes

Whenever there is a temperature difference within one medium or between two media, heat transfer occurs. We distinguish between three types of heat transfer, namely *thermal convection*, *thermal radiation* and *thermal conduction*. Each of these three modes can be described by its own appropriate rate equation. In particular, we can use them to determine the amount of energy that is transported per unit time. The aforementioned types of heat transfer can occur both individually and in combination. We distinguish:

*Convection*
This mode of heat transfer is substance-related. It describes the process of heat getting carried away by moving fluid. By *Newton's law of cooling*, we can quantify it by:

$$\boldsymbol{q_{cv}} = h(T_s - T_f) \quad \left[\frac{\mathrm{W}}{\mathrm{m}^2}\right] \tag{2.3}$$

where $T_s$ denotes the absolute temperature of the surface and $T_f$ denotes the temperature of the fluid. So the convective heat flux $q_{cv}$ is proportional to the temperature difference with a proportionality constant $h$ whose SI unit is given by $\frac{\mathrm{W}}{\mathrm{m}^2\mathrm{K}}$. We call $\boldsymbol{h}$ the *convective heat transfer coefficient* or the *film coefficient*.

*Radiation*
This mode of heat transfer is found in each matter at a non-zero temperature and requires no conduction medium (in contrast to the other two modes). It basically relies on emitting electromagnetic energy by a process of electromagnetic radiation. The intensity of this energy flux depends on the body's temperature and the nature of its surface. The maximal flux emitted by a body is given by the *Stefan-Boltzmann law*, namely:

$$\boldsymbol{q_{rd}} = \sigma_{SB}T_s^4 \quad \left[\frac{\mathrm{W}}{\mathrm{m}^2}\right] \tag{2.4}$$

where $T_s$ is the absolute temperature of the surface and $\boldsymbol{\sigma_{SB}} = 5.67 \times 10^{-8}\frac{\mathrm{W}}{\mathrm{m}^2\mathrm{K}^4}$ is the *Stefan-Boltzmann constant*. This much energy could only be emitted by a perfect radiator, which we call a *blackbody*. A blackbody absorbs all energy that reaches it. For a real surface, we need to weaken it down to:

$$\boldsymbol{q_{rd}} = \varepsilon\sigma_{SB}T_s^4 \quad \left[\frac{\mathrm{W}}{\mathrm{m}^2}\right] \tag{2.5}$$

where $\boldsymbol{\varepsilon}$ denotes the *emissivity* of the material, which is a parameter that characterizes the radiative properties of the surface of the material. It indicates how efficiently the surface emits compared with a blackbody.

*Conduction*

This mode of heat transfer describes the phenomena of heat transfer between objects by direct contact caused by a temperature difference. Heat conduction is described by *Fourier's law*, which reads in the one-dimensional case as:

$$\boldsymbol{q_{cd}} = -\kappa \frac{\partial T}{\partial x} \quad \left[ \frac{\text{W}}{\text{m}^2} \right] \tag{2.6}$$

where $\kappa$ denotes the thermal conductivity. Note that the minus sign corresponds to the direction of the flux, since heat is transferred in the direction of decreasing temperature.

Since the induced temperature changes in most of the photothermal experiments (and especially in the photothermal measurement of layer thicknesses) are small, it is merely necessary to consider heat conduction. For that reason, we focus on this phenomenon by the forthcoming derivation of the *heat diffusion equation*, which describes heat conduction.

### 2.2.2 The Heat Diffusion Equation

The surface temperature distribution of a medium is determined by solving a certain partial differential equation which arises from the rate equations just derived, as well as additional boundary conditions in the form of a certain heat input at the surface of the media. We call this particular equation the *heat diffusion equation* and derive it as follows.

Consider the following figure:
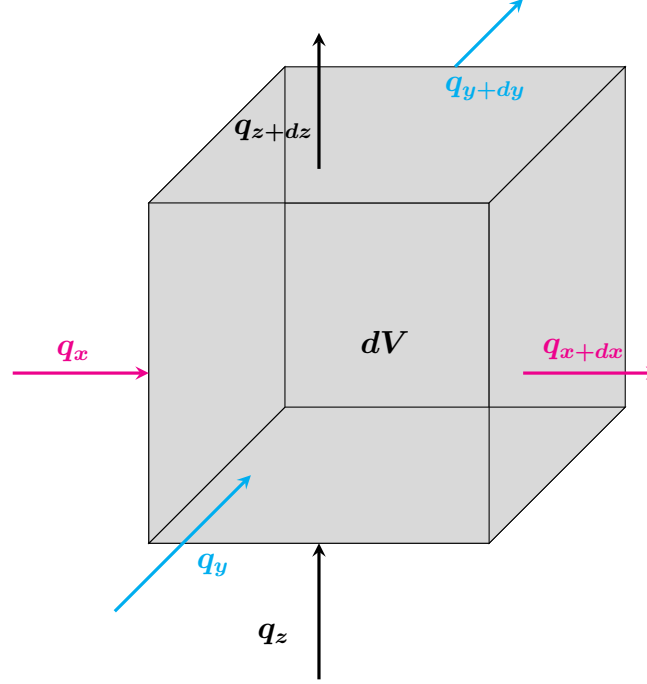


Figure 4: Differential control volume element for conduction analysis, see [12, p. 10]

Recall the *energy conservation principle* yielding:

>  *The total energy of an isolated system remains constant, it is conserved over time.*

Applying this principle to the above fluxes of thermal energy into and out of the volume element $dV$, of dimension $dx, dy$ and $dz$, we obtain the following expression:

$$Q_{in} + Q_{gen} - Q_{out} = Q_{st}, \tag{2.7}$$

where

$$\boldsymbol{Q_{in}} \coloneqq q_x + q_y + q_z$$

denotes the *rate of energy flow into* $dV$,

$$\boldsymbol{Q_{gen}} \coloneqq \dot{g} dx\, dy\, dz$$

denotes the *rate of energy generation* in $dV$,

$$\boldsymbol{Q_{out}} \coloneqq q_{x+dx} + q_{q+dy} + q_{z+dz}$$

denotes the *rate of energy flow out* of $dV$ and

$$\boldsymbol{Q_{st}} := \rho c \frac{\partial T}{\partial t} dx \; dy \; dz$$

denotes the *rate of energy storage* in $dV$. Remark that the quantity $\dot{g}$ describes the *rate of energy generation per unit volume* in the medium. Taking these four expressions into account and plugging them into Equation (2.7), we obtain the following term:

$$q_x + q_y + q_z + \dot{g} dx \; dy \; dz - q_{x+dx} - q_{y+dy} - q_{z+dz} = \rho c \frac{\partial T}{\partial t} dx \; dy \; dz.$$

By applying Fourier's law (2.6) for each direction $x, y$ and $z$, we can describe the heat fluxes entering the body as:

$$q_x = -\kappa \; dy \; dz \left. \frac{\partial T}{\partial x} \right|_x, \quad q_y = -\kappa \; dx \; dz \left. \frac{\partial T}{\partial y} \right|_y, \quad q_z = -\kappa \; dx \; dy \left. \frac{\partial T}{\partial z} \right|_z.$$

Doing the same for the heat fluxes leaving the body combined with a Taylor expansion yields then:

$$q_{x+dx} = q_x + \frac{\partial q_x}{\partial x} \; dx, \quad q_{y+dy} = q_y + \frac{\partial q_y}{\partial y} \; dy, \quad q_{z+dz} = q_z + \frac{\partial q_z}{\partial z} \; dz.$$

Applying again the *energy conservation principle* and simplifying the expression, we obtain the following equation:

$$\frac{\partial}{\partial x} \left( \kappa \; dy \; dz \; \frac{\partial T}{\partial x} \right) dx + \frac{\partial}{\partial y} \left( \kappa \; dx \; dz \; \frac{\partial T}{\partial y} \right) dy + \frac{\partial}{\partial z} \left( \kappa \; dx \; dy \; \frac{\partial T}{\partial z} \right) dz$$
$$+ \dot{g} \; dx \; dy \; dz = \rho c \frac{\partial T}{\partial t} \; dx \; dy \; dz \tag{2.8}$$

which denotes the basic form of the *heat diffusion equation* (in Cartesian co-ordinates). Solving this equation yields the temperature distribution $T(x, y, z)$ as a function of time. In simple terms, the statement of the heat diffusion equation is:

*The sum of the net rate of heat conduction into one volume element and the heat generation rate within the element at any point in a medium must equal the rate of change of the thermal energy stored at that point.*

We call such a solution of this equation a *thermal wave*. In a more physical way, a thermal wave describes the temporal as well as the spatial propagation of a temperature modulation (compare to [14]). In the subsequent subsection, we will go into more detail about the generation of such waves.

Depending on some extra information that is set, the heat diffusion equation can be simplified to the following four special cases:

**1** Assume that the medium is homogeneous, and its thermal conductivity is isotropic, i.e., independent of the direction. Then the heat differential equation reads as:

$$\frac{\partial^2 T}{\partial x^2} + \frac{\partial^2 T}{\partial y^2} + \frac{\partial^2 T}{\partial z^2} + \frac{\dot{g}}{\kappa} = \frac{1}{\alpha} \frac{\partial T}{\partial t}. \tag{2.9}$$

**2** Assume that the medium is homogeneous and there is no internal heat generation. Then the heat diffusion equation simplifies to:

$$\frac{\partial^2 T}{\partial x^2} + \frac{\partial^2 T}{\partial y^2} + \frac{\partial^2 T}{\partial z^2} = \frac{1}{\alpha}\frac{\partial T}{\partial t}. \tag{2.10}$$

We call this equation the *Fourier equation* or the *heat diffusion equation*.

**3** Assume that the medium is homogeneous, and we are in steady-state with internal heat generation. Then the heat diffusion equation reads as:

$$\frac{\partial^2 T}{\partial x^2} + \frac{\partial^2 T}{\partial y^2} + \frac{\partial^2 T}{\partial z^2} + \frac{g(x,y,z)}{\kappa} = 0. \tag{2.11}$$

We call it the *Poisson equation*.

**4** Assume that we are in steady-state without internal heat generation. Then the heat diffusion equation simplifies as:

$$\frac{\partial^2 T}{\partial x^2} + \frac{\partial^2 T}{\partial y^2} + \frac{\partial^2 T}{\partial z^2} = 0, \tag{2.12}$$

which we call the *Laplace equation*.

In this thesis, depending on the setup, we either consider isotropic, homogeneous media with no internal heat generation or a combination of such media in form of a system of layers of such materials. This means that the Fourier equation is indispensable for us. As noted in the previous subsection, the thermal diffusivity finds great importance in this case.

### 2.2.3 Thermal Wave Generation

As previously introduced, thermal waves are mathematically nothing else than solutions of the heat diffusion equation. Based on the type of the heat input at the surface of the medium which thus provides us with the appropriate boundary conditions, the surface temperature distribution is influenced and the generation of waves is determined. The most common type of excitation is a periodic, planar energy input by high-performance laser beams of a single specific excitation frequency, i.e., lock-in excitation.

For the sake of simplicity, we firstly consider an isotropic homogeneous semi-infinite (that means an infinite extension of the medium in the x-direction) medium $M$, which is described by the following figure:
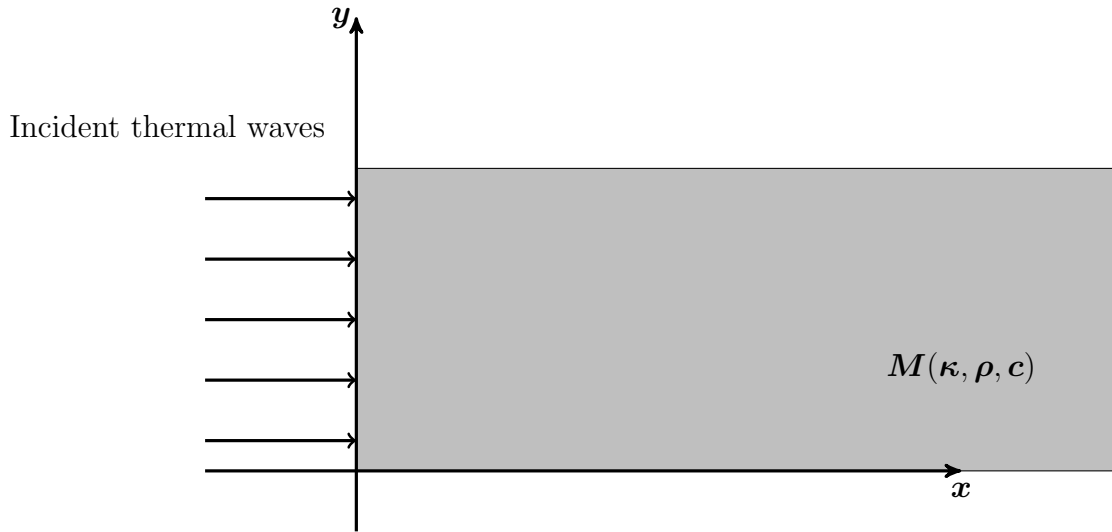


Figure 5: Thermal wave generation and propagation in a semi-infinite medium

We assume that the heated surface occupies the $y - z$-plane at $x = 0$. Consequently, to obtain the temperature distribution on the surface of the medium, we must solve the Fourier equation, which reduces to the one-dimensional case. This means that we have to solve the following equation:

$$\frac{\partial^2 T}{\partial x^2} = \frac{1}{\alpha}\frac{\partial T}{\partial t}, \quad x, t > 0 \tag{2.13}$$

where we need to specify the boundary conditions at first. We choose to excite the medium's surface with a plane harmonic, thus temporal heating of modulation frequency $\omega := 2\pi f$ for some frequency $f$ and source intensity $Q_0$ which can be described by an excitation term of the following form:

$$\frac{Q_0}{2}\left[1 + \cos(\omega t)\right],$$

yielding the generation of thermal waves on the inside of the medium.

Since the periodic thermal energy is subjected to conduction into the solid, by using

the appropriate rate equation, we obtain the following boundary condition on the surface of the medium:

$$
\begin{aligned}
-\kappa\frac{\partial T}{\partial x} &= \mathrm{Re}\left\{\frac{Q_0}{2}\left[1 + \exp\left(i\omega t\right)\right]\right\} \\
&= \frac{Q_0}{2}\left[1 + \cos(\omega t)\right] \\
&= \underbrace{\frac{Q_0}{2}}_{\text{dc component}} + \underbrace{\frac{Q_0}{2}\cos(\omega t)}_{\text{ac component}}, \quad x = 0, t > 0.
\end{aligned}
$$

Neglecting the dc component for a moment, since this quantity will not be relevant in the later applications, and applying an exponential approach, we obtain the condition:

$$
T(x, t) = \mathrm{Re}\left[T(x)\exp(i\omega t)\right].
$$

Plugging it into Equation (2.13), we end up at:

$$
\exp(i\omega t)\left(\frac{\partial^2 T(x)}{\partial x^2} - \frac{i\omega}{\alpha}T(x)\right) = 0.
$$

Taking into account that $T(x)$ must be finite for $x$ tending to infinity, we receive the equation's solution which is given as:

$$
T(x, t) = \frac{Q_0}{2\kappa\sigma}\exp(-\sigma x + i\omega t), \quad \sigma := (1 + i)\sqrt{\frac{\omega}{2\alpha}}. \tag{2.14}
$$

By multiplying the equation with $1 = \frac{i+1}{\sqrt{2}}\exp\left(-\frac{\pi}{4}\right)$ and simplifying it further, we obtain a more significant expression given by:

$$
\boldsymbol{T}(x, t) = \frac{Q_0}{2\sqrt{\rho c \kappa \omega}}\exp\left(-x\sqrt{\frac{\omega}{2\alpha}}\right)\exp\left[i\left(\omega t - x\sqrt{\frac{\omega}{2\alpha}} - \frac{\pi}{4}\right)\right] \tag{2.15}
$$

which is similar to that obtained for the amplitude of an electromagnetic wave in the surface skin depth of an electrical conductor. This quantity describes a thermal wave with wavelength:

$$
\boldsymbol{\lambda} := 2\pi\sqrt{\frac{2\alpha}{\omega}} \tag{2.16}
$$

and attenuation constant:

$$
\sqrt{\frac{2\alpha}{\omega}}
$$

which are coupled together by:

$$
\sqrt{\frac{2\alpha}{\omega}} = \frac{\lambda}{2\pi}.
$$

In this context, we define the *thermal diffusion length* (see Section 1.2.3) as the quantity:

$$\boldsymbol{\mu} := \sqrt{\frac{2\alpha}{\omega}} = \sqrt{\frac{2\kappa}{\rho\omega c}} \tag{2.17}$$

which corresponds to the electromagnetic skin depth. Remark that $\mathrm{Re}(\sigma) = \mathrm{Im}(\sigma) = \frac{1}{\mu}$. The thermal diffusion length controls the penetration depth of the thermal waves into the material. Thus, note that thermal waves are heavily damped with a decay constant equal to this thermal diffusion length $\mu$. Remark that for small thermal conductivity, $\kappa$ or for high density $\rho$ or high specific heat capacity $c$, the thermal waves do not enter that deep into the material. In contrast, by decreasing the modulation frequency $\omega$, we obtain a deeper penetration of the thermal waves into the material. This phenomenon is used in the photothermal measurement of layer thicknesses because via this property one can control the reach of the thermal waves into the material, which is quite useful. However, from Equation (2.17) it follows that the thermal diffusion length is always smaller than the wavelength, resulting in the fact that the thermal wave never occurs as a whole wave train.

Furthermore, note that there occurs a progressive phase shift between the temperature at the surface and a point $x$ laying on the propagating thermal wave in the material, namely:

$$\varphi = -\frac{x}{\mu} - \frac{\pi}{4}. \tag{2.18}$$

Thus, at the surface there is an expressive phase difference of $-45$ deg. between the excitation source and the resulting surface temperature.

## 2.3   Reflection and Refraction Effects

In the previous subsection, thermal waves are introduced. Similar to electromagnetic and acoustic waves, reflection, and refraction effects also occur for this type of waves. Subsequently, these properties of thermal waves are explained and exploited. We mainly refer to [12, 15, 16].

In analogy to electromagnetic and acoustic waves, thermal waves are reflected as well as refracted at interfaces between materials possessing different thermophysical properties. Exploiting the heat diffusion equation, we firstly obtain an impressive representation of the *thermal wave reflection coefficient*, which is a parameter that determines how much of the incident wave is being reflected at the boundary and secondly one of the *thermal wave transmission coefficient* which determines how much of the incident thermal wave is being transmitted by the material.

For the sake of simplicity, consider two media $M_1$ (that is typically a certain coating) and $M_2$ (that is typically a certain substrate) with different thermophysical properties, separated by the $x = 0$ plane. Assume that the incident thermal wave is characterized by the angle $\theta_i$, the reflected thermal wave is characterized by the angle $\theta_r$ and the refracted thermal wave that occurs by transmission, is characterized by the angle $\theta_t$ as portrayed by the following picture:
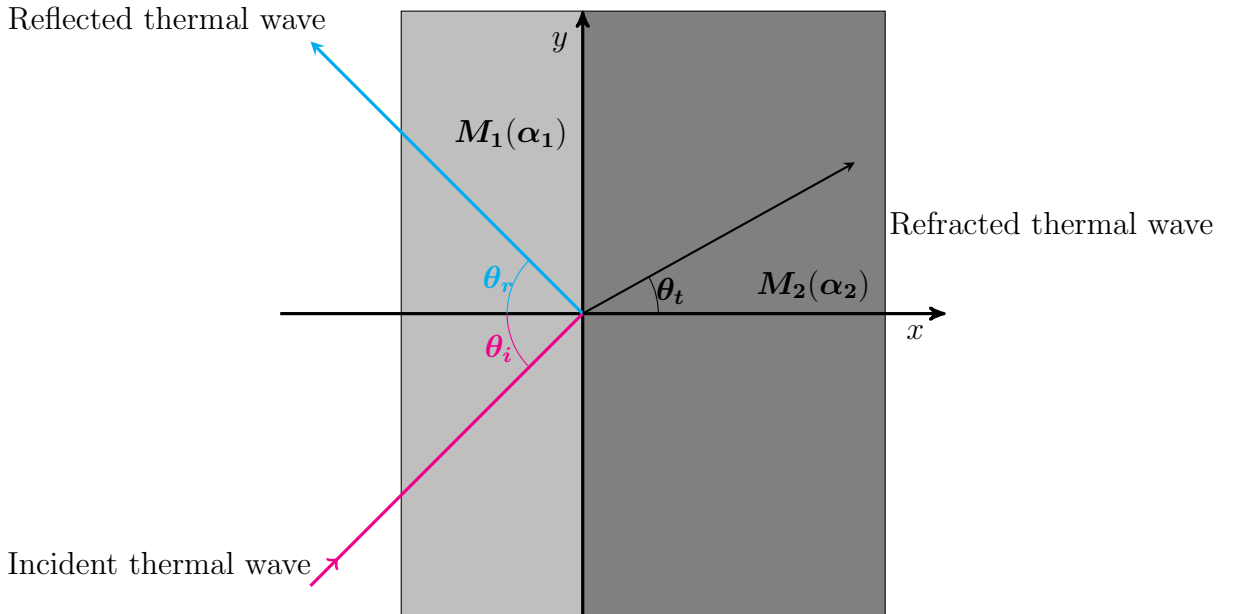


Figure 6: Reflection and refraction of thermal waves at a media boundary

Taking these assumptions into account, we obtain the following expressions that describe

the different thermal waves:

$$
\begin{aligned}
\boldsymbol{T_i}(x, y, t) &= A_0 \exp\left(\sigma_1 x \cos\theta_i + \sigma_1 y \sin\theta_i + i\omega t\right), \\
\boldsymbol{T_r}(x, y, t) &= A_0 R \exp\left(-\sigma_1 x \cos\theta_r + \sigma_1 y \sin\theta_r + i\omega t\right), \\
\boldsymbol{T_t}(x, y, t) &= A_0 T \exp\left(\sigma_2 x \cos\theta_t + \sigma_2 y \sin\theta_t + i\omega t\right), \\
\boldsymbol{\sigma_1} &:= (1+i)\sqrt{\frac{\omega}{2\alpha_1}}, \quad \boldsymbol{\sigma_2} := (1+i)\sqrt{\frac{\omega}{2\alpha_2}}
\end{aligned}
\tag{2.19}
$$

where $T_i$ denotes the incident, $T_r$ the reflected and $T_t$ the transmitted thermal wave and $\sigma_1, \sigma_2$ the wave vectors for $M_1$, $M_2$, respectively. Remark that the quantity $A_0$ denotes the initial amplitude of the incident thermal wave, $R$ denotes the *thermal wave reflection coefficient* and $T$ denotes the *thermal wave transmission coefficient* at the interface $x = 0$. We want to describe and characterize these two important properties in detail.

Firstly, since the temperature at the interface $x = 0$ has to be continuous (thus, the temperature on both sides of the boundary has to be equal), i.e., $T_i + T_r = T_t$ has to hold, we obtain the following condition:

$$
A_0 \exp\left(\sigma_1 y \sin\theta_i\right) + A_0 R \exp\left(\sigma_1 y \sin\theta_r\right) = A_0 T \exp\left(\sigma_2 y \sin\theta_t\right).
$$

Noting that this equation has to hold true for all positions $y$ across the interface plane which is fulfilled only if the waves are in phase, the exponents in the equation must all be equal leading to the constraint:

$$
\sigma_1 y \sin\theta_i = \sigma_1 y \sin\theta_r = \sigma_2 y \sin\theta_t.
$$

From the first equality we are able to derive the *law of reflection*, namely:

$$
\theta_i = \theta_r
\tag{2.20}
$$

and from the second equality we obtain the *law of refraction*, namely:

$$
\sigma_1 \sin\theta_i = \sigma_2 \sin\theta_t
\tag{2.21}
$$

both of which are formulated completely analogous for electromagnetic and acoustic waves.

Secondly, consider the following three fluxes:

$$
q_i = -\kappa_1 \frac{\partial T_i}{\partial x}, \quad q_r = -\kappa_1 \frac{\partial T_r}{\partial x}, \quad q_t = -\kappa_2 \frac{\partial T_t}{\partial x}.
\tag{2.22}
$$

Plugging Equation (2.19) into Equations (2.22) and applying the law of reflection, we

obtain:

$$
\begin{aligned}
q_i &= -\kappa_1 \frac{\partial T_i}{\partial x} \left( A_0 \exp\left( \sigma_1 x \cos\theta_i + \sigma_1 y \sin\theta_i + i\omega t \right) \right) \\
&= -\kappa_1 \sigma_1 \cos\theta_i A_0 \exp\left( -\sigma_1 x \cos\theta_i - \sigma_1 y \sin\theta_i + i\omega t \right), \\
q_r &= -\kappa_1 \frac{\partial T_r}{\partial x} \left( A_0 R \exp\left( -\sigma_1 x \cos\theta_r + \sigma_1 y \sin\theta_r + i\omega t \right) \right) \\
&= \kappa_1 \sigma_1 \cos\theta_r A_0 R \exp\left( -\sigma_1 x \cos\theta_r + \sigma_1 y \sin\theta_r + i\omega t \right) \\
&= \kappa_1 \sigma_1 \cos\theta_i A_0 R \exp\left( -\sigma_1 x \cos\theta_i + \sigma_1 y \sin\theta_i + i\omega t \right), \\
q_t &= -\kappa_2 \frac{\partial T_t}{\partial x} \left( A_0 T \exp\left( \sigma_2 x \cos\theta_t + \sigma_2 y \sin\theta_t + i\omega t \right) \right) \\
&= -\kappa_2 \sigma_2 \cos\theta_t A_0 T \exp\left( \sigma_2 x \cos\theta_t + \sigma_2 y \sin\theta_t + i\omega t \right).
\end{aligned}
\tag{2.23}
$$

Since the flux at the interface should also be continuous, i.e., $q_i = q_r + q_t$ has to hold, we generally obtain:

$$
\kappa_1 \sigma_1 \cos\theta_i = R\kappa_1 \sigma_1 \cos\theta_i - T\kappa_2 \sigma_2 \cos\theta_t.
$$

Making use of the fact that $T = 1 + R$ at $y = 0$, the thermal wave reflection coefficient attains the following form:

$$
\boldsymbol{R} = \frac{\kappa_1 \sigma_1 \cos\theta_i - \kappa_2 \sigma_2 \cos\theta_t}{\kappa_1 \sigma_1 \cos\theta_i + \kappa_2 \sigma_2 \cos\theta_t} = \frac{\cos\theta_i - b\cos\theta_t}{\cos\theta_i + b\cos\theta_t}
\tag{2.24}
$$

and the thermal transmission coefficient attains the form:

$$
\boldsymbol{T} = \frac{2\kappa_1 \sigma_1 \cos\theta_i}{\kappa_1 \sigma_1 \cos\theta_i + \kappa_2 \sigma_2 \cos\theta_t} = \frac{2\cos\theta_i}{\cos\theta_i + b\cos\theta_i},
\tag{2.25}
$$

where we define the *thermal refraction index*:

$$
\boldsymbol{b} = \frac{\kappa_2 \sigma_2}{\kappa_1 \sigma_1} = \frac{\sqrt{\kappa_2 \rho_2 c_2}}{\sqrt{\kappa_1 \rho_1 c_1}} = \frac{\varepsilon_2}{\varepsilon_1}
\tag{2.26}
$$

as the ratio between the thermal effusivities of $M_2$ and $M_1$ respectively. Loosely speaking, this property $b$ characterizes the thermal "mismatch" between the two media $M_1$ and $M_2$ and thus characterizes the occurring reflection and refraction effects. Note that we will only consider vertical illumination of the material's surface, thus, $\theta_i = \theta_r = 0$, simplifying the expressions for the thermal reflection coefficient and the thermal transmission coefficient at the surface $x = 0$ to:

$$
R = \frac{1 - b}{1 + b} = \frac{\varepsilon_1 - \varepsilon_2}{\varepsilon_1 + \varepsilon_2}, \quad T = \frac{2}{1 + b} = \frac{2\varepsilon_2}{\varepsilon_1 + \varepsilon_2},
\tag{2.27}
$$

respectively. Naturally, it follows:

$$
T = 1 + R.
$$

Notice that the thermal reflection coefficient and the thermal transmission coefficient only depend on the thermophysical properties of the materials. Thus, it is crucial that the sample that is being illuminated is absorbing optical energy and that these properties are sufficiently different between two media in order to actually obtain reflection effects. Also note that this is again analogous to electromagnetic and acoustic waves.

# 3   Mathematical Modeling of the Inverse Problem

In this section, all acquired knowledge from the previous sections flows together, leading to the introduction of the inverse problem of *photothermal measurement of layer thicknesses in multilayered systems* using lock-in thermography. For that reason, we define the fitting forward operators, namely calculating the phase angle for given layer thicknesses. Further, utilizing those, we define the corresponding inverse operators, yielding the mathematical modeling of said inverse problem.

## 3.1   Modeling of the Forward Problem

After introducing the reflection as well as the refraction effects that occur for thermal waves, we specify on a two layered system of different materials and exploit the appearing interference effects before we then expand it to a $n$ layered system of different materials for a natural number $n \in \mathbb{N}$, $n \geq 2$. These observations provide us in each case with a formula specifying the complex surface temperature of the system. Subsequently, using Euler's formula, we then obtain the amplitude as well as the phase angle of this quantity. We mainly refer to [12].

Consider the following system of two layers of media $M_1$ and $M_2$, possessing different thermophysical properties:

Transmitted thermal waves
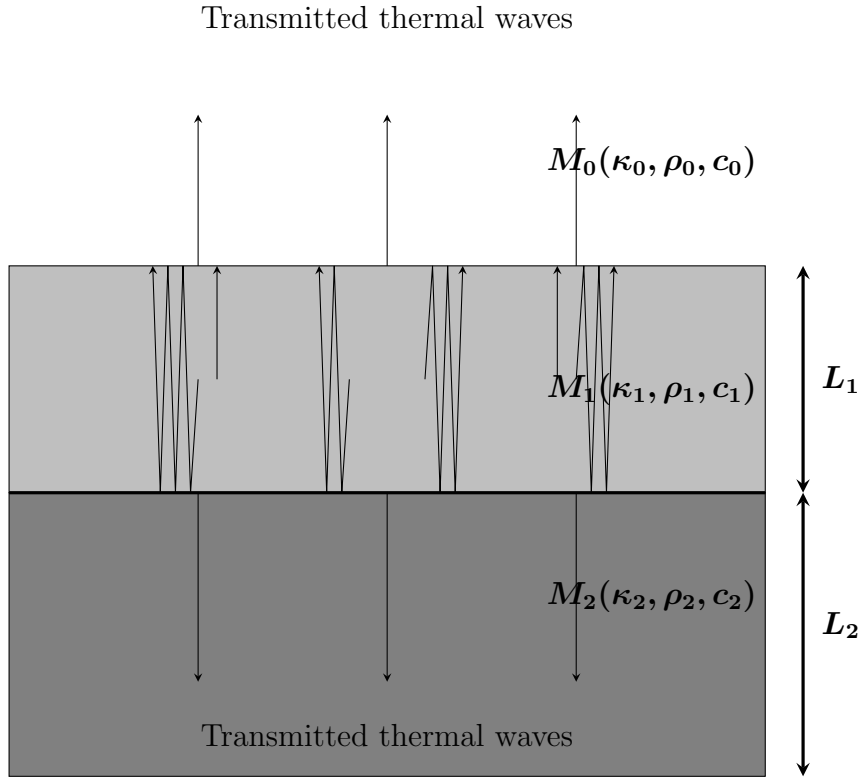


Figure 7: Thermal wave interference in the layer for a two layered system of materials

Assume that both media $M_1$ and $M_2$ have homogeneous thermophysical properties and that $M_1$ is of thickness $L_1$ and $M_2$ is of thickness $L_2$. Furthermore, assume that $M_2$ is

*thermally thick.* That means that it is much thicker than the thermal diffusion length $\mu_2$, i.e., it holds that $L_2 >> \mu_2$. Via this assumption, we interpret the system as semi-infinite (compare to Section 2.2.3). Moreover, assume that the whole system is exposed to air, which we denote by $M_0$. Suppose that the surface is illuminated by a plane, normal and periodic heating.

The single wave trains that are generated near the surface propagate towards the interface between the two media and back towards the surface of $M_1$. When reaching the boundaries, the waves are partially reflected and transmitted. Thus, thermal wave interference occurs between these different wave trains. Mathematically, that means that the waves that arrive at the surface sum up, providing the surface temperature. We distinguish two cases:

**(1)** Consider waves that are first reflected from the boundary between $M_0$ and $M_1$ as described by the following picture:
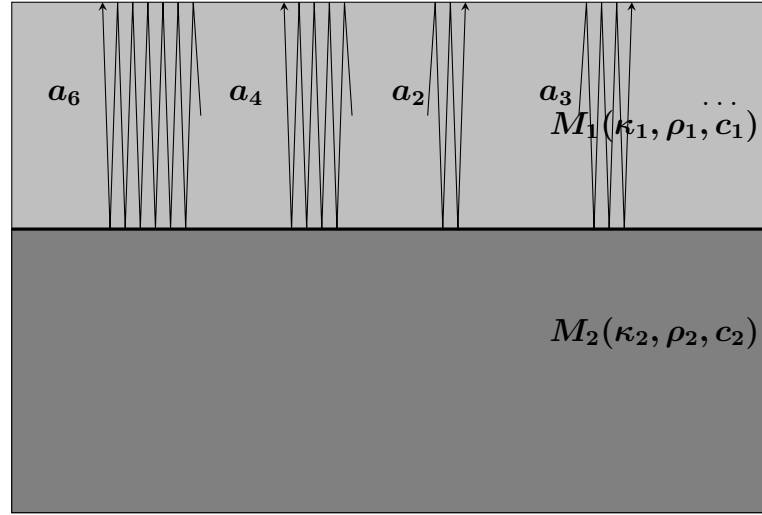


Figure 8: Waves that are reflected first at the boundary between $M_0$ and $M_1$

Denote by $a_n$ the $n^{\text{th}}$ reflection order wave, by $R_0(R_1)$ the reflection coefficient at the boundary between $M_0$ and $M_1(M_1$ and $M_2)$ as well as by $T_0(T_0')$ the transmission coefficient at the boundary between $M_0$ and $M_1$ in the downward (upward) direction. Since the single wave trains are reflected at the boundary "infinitely" often, we

obtain the following series corresponding to the surface temperature:

$$
\begin{aligned}
\sum_{n=0}^{\infty} a_n &= T_0 A_0 \sum_{n=1}^{\infty} \left(1 + R_0^n R_1^n \exp\left(-2n\sigma_1 L_1\right)\right) \\
&= T_0 A_0 \sum_{n=0}^{\infty} R_0^n R_1^n \exp\left(-2n\sigma_1 L_1\right) \\
&= T_0 A_0 \sum_{n=0}^{\infty} \left[R_0 R_1 \exp\left(-2\sigma_1 L_1\right)\right]^n \\
&= T_0 A_0 \frac{1}{1 - R_0 R_1 \exp\left(-2\sigma_1 L_1\right)} \\
&= \frac{T_0 A_0}{1 - R_0 R_1 \exp\left(-2\sigma_1 L_1\right)},
\end{aligned}
\tag{3.1}
$$

where we use the geometric series formula, since clearly $|R_0 R_1 \exp\left(-2\sigma_1 L_1\right)| < 1$ holds true.

**(2)** Consider waves that are first reflected from the boundary between $M_1$ and $M_2$ as described by the following picture:
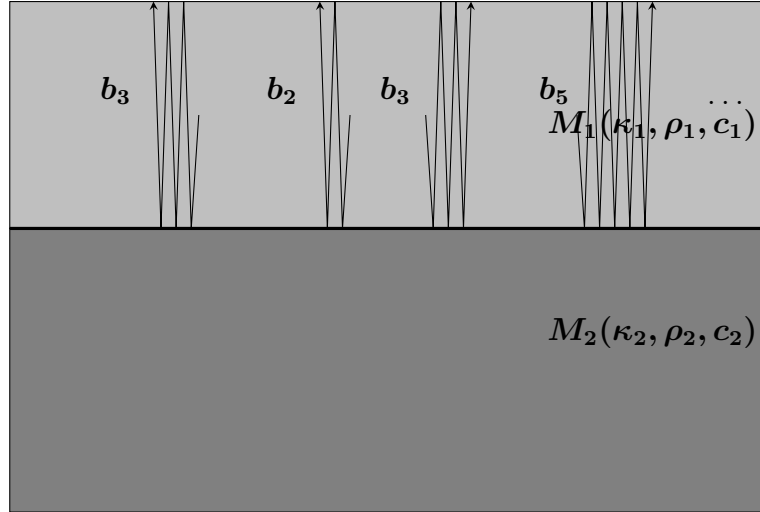


Figure 9: Waves that are reflected first at the boundary between $M_1$ and $M_2$

Denote by $b_n$ the $n^{\text{th}}$ reflection order wave. Analogous to the first case, we obtain the following expression for the amplitude of the wave corresponding to the surface

temperature:

$$
\begin{aligned}
\sum_{n=0}^{\infty} b_n &= T_0 A_0 R_1 \exp\left(-2\sigma_1 L_1\right) \sum_{n=1}^{\infty} \left(1 + R_0^n R_1^n \exp\left(-2n\sigma_1 L_1\right)\right) \\
&= T_0 A_0 R_1 \exp\left(-2\sigma_1 L_1\right) \sum_{n=0}^{\infty} R_0^n R_1^n \exp\left(-2n\sigma_1 L_1\right) \\
&= T_0 A_0 R_1 \exp\left(-2\sigma_1 L_1\right) \sum_{n=0}^{\infty} \left[R_0 R_1 \exp\left(-2\sigma_1 L_1\right)\right]^n \\
&= T_0 A_0 R_1 \exp\left(-2\sigma_1 L_1\right) \frac{1}{1 - R_0 R_1 \exp\left(-2\sigma_1 L_1\right)} \\
&= \frac{T_0 A R_1 \exp\left(-2\sigma_1 L_1\right)}{1 - R_0 R_1 \exp\left(-2\sigma_1 L_1\right)},
\end{aligned}
\tag{3.2}
$$

where we use the geometric series formula, since clearly $\left|R_0 R_1 \exp\left(-2\sigma_1 L_1\right)\right| < 1$ holds true.

By summing up both of these series, we obtain the temperature amplitude for the thermal wave interference expression on the surface, namely:

$$
\begin{aligned}
\sum_{n=0}^{\infty} a_n + \sum_{n=0}^{\infty} b_n &= \frac{T_0 A_0}{1 - R_0 R_1 \exp\left(-2\sigma_1 L_1\right)} + \frac{T_0 A_0 R_1 \exp\left(-2\sigma_1 L_1\right)}{1 - R_0 R_1 \exp\left(-2\sigma_1 L_1\right)} \\
&= T_0 A_0 \left[\frac{1 + R_1 \exp\left(-2\sigma_1 L_1\right)}{1 - R_0 R_1 \exp\left(-2\sigma_1 L_1\right)}\right] =: \tilde{\boldsymbol{T}}(x = 0).
\end{aligned}
\tag{3.3}
$$

This provides us with the following expression for the time dependent temperature at the surface:

$$
\boldsymbol{T}(x = 0, t) = \tilde{T}(x = 0) \exp\left[i(\omega t - \frac{\pi}{4})\right].
\tag{3.4}
$$

Notice that the phase shift in this formula, given by $\frac{\pi}{4}$, follows from Equation (2.18).

Since the wave vector $\sigma_1 = (1 + i)\sqrt{\frac{\omega}{2\alpha_1}} = (1 + i)\frac{1}{\mu_1}$ is complex, implying that the temperature amplitude is complex valued, we can split it into its real and its imaginary part. That provides us with an expression in polar co-ordinates. For that reason set:

$$
\sigma_1 = \text{Re}(\sigma_1) + i\text{Im}(\sigma_1) = \frac{1}{\mu_1} + i\frac{1}{\mu_1} := \sigma_1' + i\sigma_1''.
$$

Hence we calculate:

$$
\begin{aligned}
&\text{Re}\left[\tilde{T}(x = 0)\right] \\
&= \frac{1 - R_0^2 R_1^2 \exp\left(-4\frac{L_1}{\mu_1}\right) + R_1 \exp\left(-2\frac{L_1}{\mu_1}\right) \cos(-2\frac{L_1}{\mu_1})\left[1 - R_1\right]}{\left[1 - R_0^2 R_1^2 \exp\left(-2\frac{L_1}{\mu_1}\right) \cos\left(-2\frac{L_1}{\mu_1}\right)\right]^2 + \left[R_0 R_1 \exp\left(-2\frac{L_1}{\mu_1}\right) \sin\left(-2\frac{L_1}{\mu_1}\right)\right]^2}
\end{aligned}
$$

and

$$\text{Im}\left[\tilde{T}(x=0)\right]$$

$$= \frac{[1+R_0]\left[R_1 \exp\left(-2\frac{L_1}{\mu}\right)\sin\left(-2\frac{L_1}{\mu_1}\right)\right]}{\left[1-R_0^2 R_1^2 \exp\left(-2\frac{L_1}{\mu_1}\right)\cos\left(-2\frac{L_1}{\mu_1}\right)\right]^2 + \left[R_0 R_1 \exp\left(-2\frac{L_1}{\mu_1}\right)\sin\left(-2\frac{L_1}{\mu_1}\right)\right]^2}.$$

Define $x := \frac{-2L_1}{\mu_1}$. Thus we obtain the amplitude $A_{\tilde{T}}$ as:

$$\boldsymbol{A_{\tilde{T}}} = \sqrt{\text{Re}\left[\tilde{T}(x=0)\right]^2 + \text{Im}\left[\tilde{T}(x=0)\right]^2}$$

$$= \frac{\sqrt{\left[1+R_1(1-R_0)\exp\left(x\right)\cos\left(x\right)-R_1^2 R_0 \exp(2x)\right]^2 + \left[R_1(1+R_0)\exp\left(x\right)\sin\left(x\right)\right]^2}}{\left[1-R_0 R_1 \exp\left(x\right)\cos\left(x\right)\right]^2 + \left[R_0 R_1 \exp\left(x\right)\sin\left(x\right)\right]^2}$$

$$(3.5)$$

as well as the phase angle $\varphi_{\tilde{T}}$ as:

$$\boldsymbol{\varphi_{\tilde{T}}} = \tan^{-1}\left[\frac{\text{Im}\left[\tilde{T}(x=0)\right]}{\text{Re}\left[\tilde{T}(x=0)\right]}\right]$$

$$= \tan^{-1}\left[\frac{[1+R_0]\left[R_1 \exp\left(x\right)\sin\left(x\right)\right]}{1+(1-R_0)R_1 \exp\left(x\right)\cos\left(x\right)-R_1^2 R_0 \exp\left(2x\right)}\right]$$

$$(3.6)$$

which provides us with an expression for the complex temperature amplitude at the surface in polar coordinates, i.e. $\tilde{T}(x=0) = A_{\tilde{T}}\exp\left(i\varphi_{\tilde{T}}\right)$. The advantage of this form is that the amplitude as well as the phase are measurable real expressions. For that reason, these quantities are used in the measuring process of layer thicknesses.

In the following figure, a number of different plots using Equations (3.5) and (3.6) are pictured:
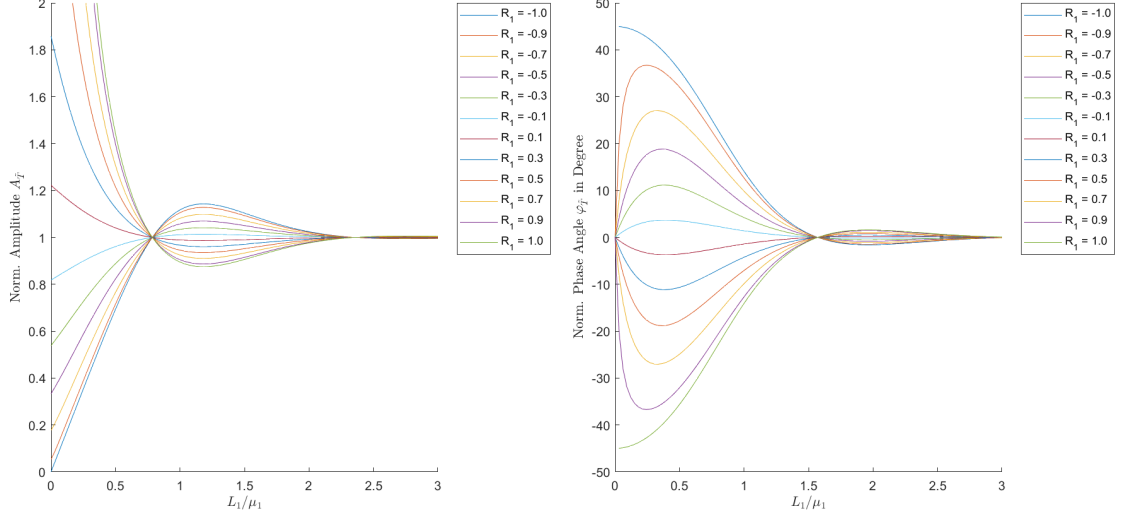


Figure 10: Normalized signal amplitude variation (left) and normalized phase angle variation (right) with normalized coating thickness for various coating/substrate reflection coefficients, see [12, p. 24]

The curves are plotted against the reduced coating thickness $\frac{L_1}{\mu_1}$ of media $M_1$ and vary through the reflection coefficient $R_1$ at the boundary of media $M_1$ and $M_2$ of values between $-1$ and $1$. Remark that the phase is normalized by subtracting an "infinitely" thick layer, i.e., $\varphi_{\tilde{T}}(L = \infty) = -45$ deg. For reasons of simplicity, the reflection coefficient $R_0$ at the surface of the system is set equal to 1. However, remark that in general it is smaller, between 0.92 and 0.95 when working with synthetic materials. Both pictures emphasize the importance of the reflection coefficient $R_1$ namely the reflection coefficient at the coating/substrate boundary. Since thermal waves are heavily damped as noted in Section 2.2.3 the bulk of the interference effects occur where the thickness is less than the thermal diffusion length $\mu_1$.

In a completely analogous way, similar formulas as the aforementioned ones can be derived for general systems consisting of $n \in \mathbb{N}$, $n \geq 2$ layers of materials. We follow this plan on the next pages by introducing an entirely new mathematical modeling, initially done in this thesis.

Consider the following system consisting of $n, n \in \mathbb{N}$ layers of media $M_1$ - $M_n$ of thicknesses $L_1$ - $L_n$:

Transmitted thermal waves
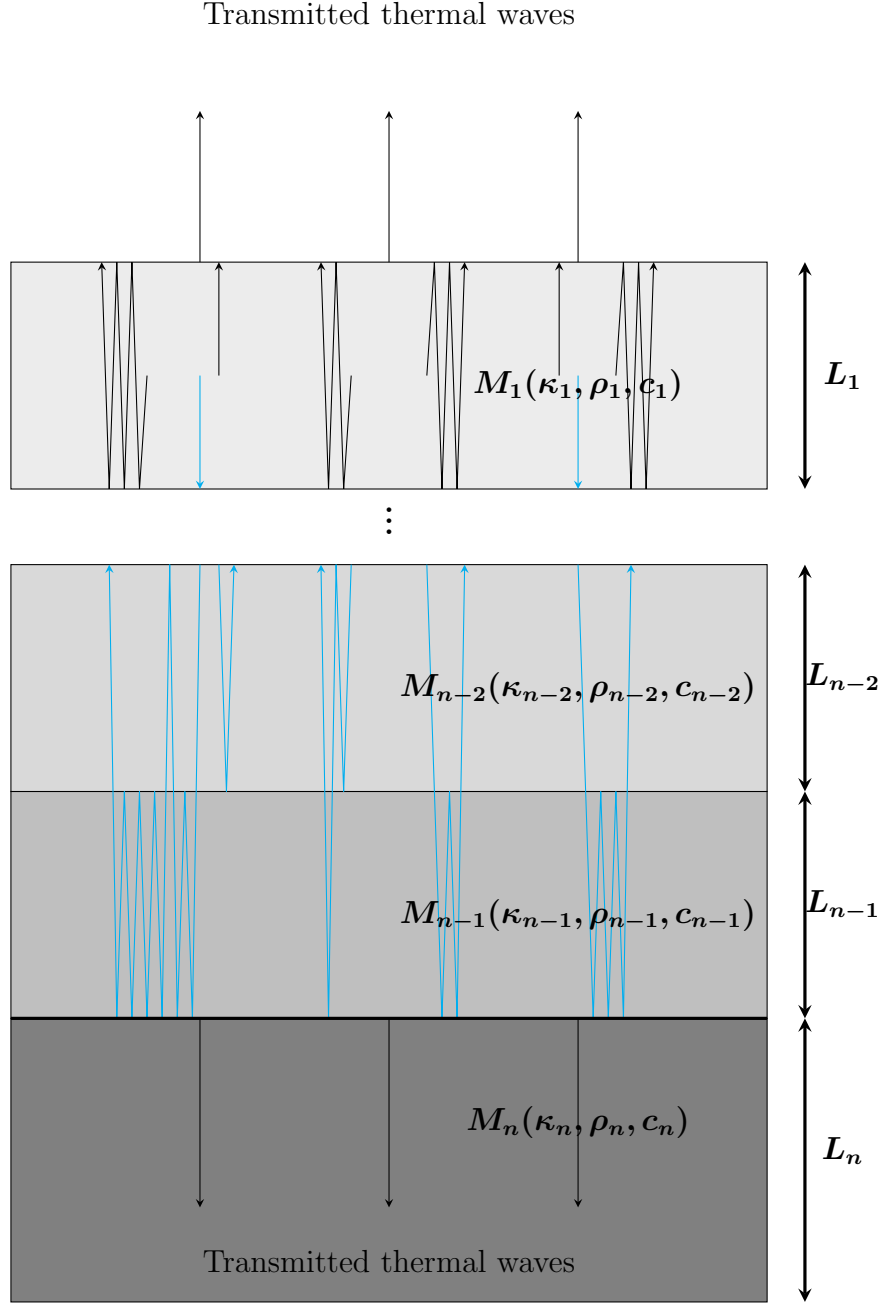


Figure 11: System of $n-1$ Layers of coating $M_1$ - $M_{n-1}$ and one Layer of substrate $M_n$

Again, medium $M_n$ is a (metallic) substrate and media $M_1$ - $M_{n-1}$ are (non-metallic) coating layers.

The difference to the two layered system can be observed by the arrows drawn in blue in the picture. Since we now have several layers and thus also several interfaces, the waves are reflected and refracted at all of these interfaces. Thus, thermal interference occurs in each layer. Mathematically, this means that we expect "more" reflection coefficients and transmission coefficients for each of the $n - 1$ interfaces in the new formula. In the following, we take a closer look at the case of two coating layers, deriving a new formula, before we then expand to the general case of $n$, $n \in \mathbb{N}$ coating layers.

Consider the following system consisting of three layers of media $M_1$ - $M_3$ of thicknesses $L_1$ - $L_3$, where $M_3$ is thermally thick:

<div align="center">Transmitted thermal waves</div>
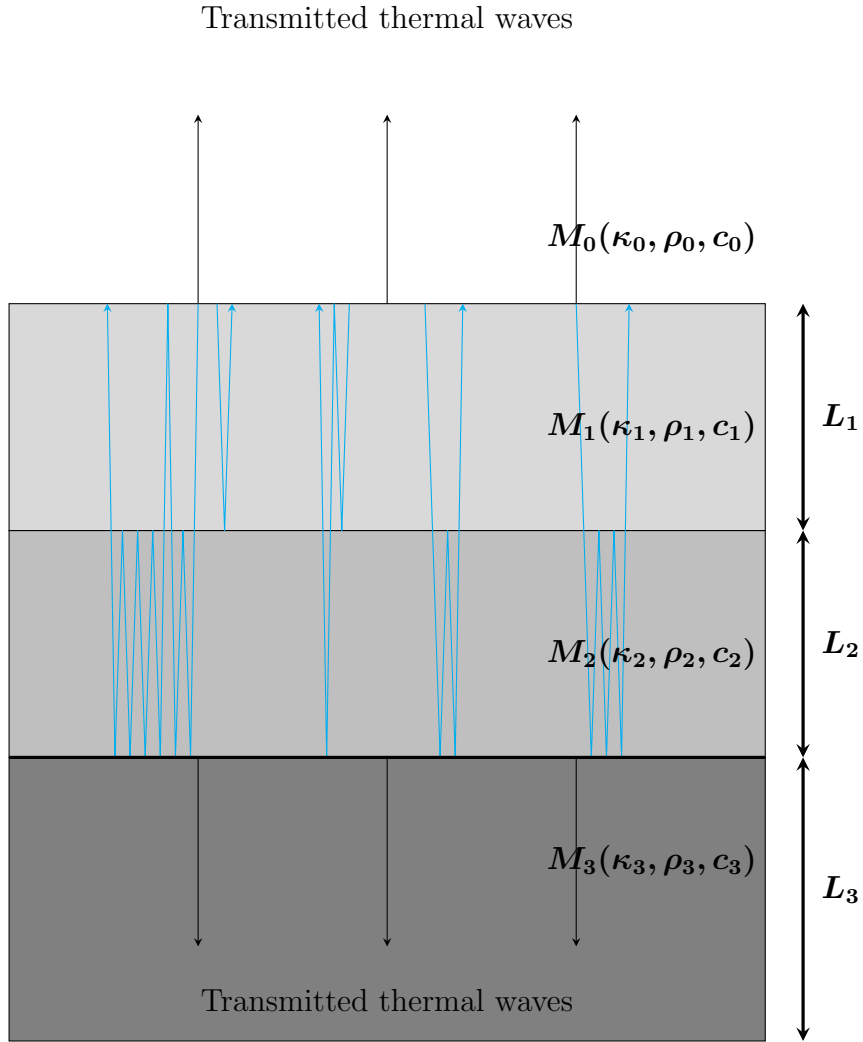


Figure 12: System of two layers of coating $M_1$ - $M_2$ and one layer of substrate $M_3$

As stated above, for a system with at least two coating layers the temperature formula introduced in Equation (3.4) is not sufficient anymore since the reflection processes in the two cases differ dramatically since before, we only had to deal with real reflection coefficients, by introducing a new layer, the process changes, and we expect a complex quantity since it is dependent on the wave vector. The main difference occurs at the

boundary of the new layer $M_2$ and the layer $M_1$. Consider the formula from Equation (3.3):

$$\tilde{T}(x = 0) = T_0 A_0 \left[ \frac{1 + R_1 \exp\left(-2\sigma_1 L_1\right)}{1 - R_0 R_1 \exp\left(-2\sigma_1 L_1\right)} \right].$$

By introducing a new layer, the reflection and refraction process expands after passing the interface between $M_1$ and $M_2$ and takes also place a level lower. Thus, interference effects occur in the new layer $M_2$ as well. This implies that the reflection coefficient $R_1$ does not suffice to describe the whole process anymore, so we need to change the expression in $R_1$ analogously to the derivation in Equation (3.1) in the following way:

$$
\begin{aligned}
\mathbf{\Gamma_1} &:= R_1 + T_1 T_1' R_2 \exp\left(-2\sigma_2 L_2\right) \left( 1 + \sum_{n=1}^{\infty} (R_1')^n R_2^n \exp\left(-2n\sigma_2 L_2\right) \right) \\
&= R_1 + T_1 T_1' R_2 \exp\left(-2\sigma_2 L_2\right) \sum_{n=0}^{\infty} \left( R_1' R_2 \exp\left(-2\sigma_2 L_2\right) \right)^n \\
&= R_1 + T_1 T_1' R_2 \exp\left(-2\sigma_2 L_2\right) \sum_{n=0}^{\infty} \left( -R_1 R_2 \exp\left(-2\sigma_2 L_2\right) \right)^n \\
&= R_1 + (1 - R_1^2) R_2 \exp\left(-2\sigma_2 L_2\right) \sum_{n=0}^{\infty} \left( -R_1 R_2 \exp\left(-2\sigma_2 L_2\right) \right)^n \\
&= R_1 + \left( R_2 \exp\left(-2\sigma_2 L_2\right) - R_1^2 R_2 \exp\left(-2\sigma_2 L_2\right) \right) \frac{1}{1 + R_1 R_2 \exp\left(-2\sigma_2 L_2\right)} \\
&= \frac{R_1 + R_1^2 R_2 \exp\left(-2\sigma_2 L_2\right)}{1 + R_1 R_2 \exp\left(-2\sigma_2 L_2\right)} + \frac{R_2 \exp\left(-2\sigma_2 L_2\right)}{1 + R_1 R_2 \exp\left(-2\sigma_2 L_2\right)} - \frac{R_1^2 R_2 \exp\left(-2\sigma_2 L_2\right)}{1 + R_1 R_2 \exp\left(-2\sigma_2 L_2\right)} \\
&= \frac{R_1 + R_2 \exp\left(-2\sigma_2 L_2\right)}{1 + R_1 R_2 \exp\left(-2\sigma_2 L_2\right)}.
\end{aligned}
\tag{3.7}
$$

Note that we used the geometric series formula, since clearly $|-R_1 R_2 \exp\left(-2\sigma_2 L_2\right)| < 1$ holds true as well as $R_j' = -R_j$, $T_j = 1 + R_j$ and thus $T_j' T_j = 1 - R_j^2$, $\quad j = 0, \ldots n-1$. We call the quantity $\Gamma_1$ the *effective reflection coefficient*. Substituting $R_1$ by $\Gamma_1$ in Equation (3.4), we end up with the following surface temperature for the three layered system:

$$
\begin{aligned}
\boldsymbol{T}(x = 0, t) &= T_0 A_0 \left[ \frac{1 + \Gamma_1 \exp\left(-2\sigma_1 L_1\right)}{1 - R_0 \Gamma_1 \exp\left(-2\sigma_1 L_1\right)} \right] \exp\left[ i \left( \omega t - \frac{\pi}{4} \right) \right] \\
&=: \tilde{\boldsymbol{T}}(x = 0) \exp\left[ i \left( \omega t - \frac{\pi}{4} \right) \right].
\end{aligned}
\tag{3.8}
$$

Once again, this expression provides us with a term for the amplitude:

$$
\boldsymbol{A_{\tilde{T}}} = \sqrt{ \text{Re}\left[ \tilde{T}(x = 0) \right]^2 + \text{Im}\left[ \tilde{T}(x = 0) \right]^2 }.
\tag{3.9}
$$

as well as a term for the phase angle:

$$
\boldsymbol{\varphi_{\tilde{T}}} = \tan^{-1} \left[ \frac{\text{Im}\left[ \tilde{T}(x = 0) \right]}{\text{Re}\left[ \tilde{T}(x = 0) \right]} \right].
\tag{3.10}
$$

yielding

$$\tilde{T}(x = 0) = A_{\tilde{T}} \exp\left(i\varphi_{\tilde{T}}\right).$$

Again, in a completely analog manner, we obtain a similar formula for an arbitrary number $n \in \mathbb{N} \cup \{0\}$ characterizing a $n + 2$ layered system by recursively defining the effective reflection coefficient $\Gamma_1$ in the following way:

**Definition 3.1** *Let $n \in \mathbb{N}$ be a natural number and let $j = n, \ldots, 1$. Let $R_j$ be the reflection coefficient at the interface between media $M_j$ and $M_{j+1}$. We define the effective reflection coefficient $\Gamma_i$ as:*

$$\Gamma_{n+1} := R_{n+1},$$
$$\boldsymbol{\Gamma_j} = \frac{R_j + \Gamma_{j+1} \exp\left(-2\sigma_{j+1}L_{j+1}\right)}{1 + R_j\Gamma_{j+1} \exp\left(-2\sigma_{j+1}L_{j+1}\right)}, \quad \sigma_j = (i+1)\sqrt{\frac{\omega}{2\alpha_j}}.$$

This then directly results in the following quantity for the surface temperature:

$$\begin{aligned}
\boldsymbol{T}(x = 0, t) &= \left[A_0 T_0 \frac{1 + \Gamma_1 \exp\left(-2\sigma_1 L_1\right)}{1 - R_0\Gamma_1 \exp\left(-2\sigma_1 L_1\right)}\right] \exp\left[i\left(\omega t - \frac{\pi}{4}\right)\right] \\
&=: \tilde{T}(x = 0) \exp\left[i\left(\omega t - \frac{\pi}{4}\right)\right].
\end{aligned} \tag{3.11}$$

Remark that for the case $n = 1$, i.e., in the three layered system we immediately obtain the formula from Equation (3.8), showing that this definition indeed provides us with a good generalization. Again from this expression we derive its amplitude:

$$\boldsymbol{A_{\tilde{T}}} = \sqrt{\mathrm{Re}\left[\tilde{T}(x = 0)\right]^2 + \mathrm{Im}\left[\tilde{T}(x = 0)\right]^2}. \tag{3.12}$$

as well as its phase angle:

$$\boldsymbol{\varphi_{\tilde{T}}} = \tan^{-1}\left[\frac{\mathrm{Im}\left[\tilde{T}(x = 0)\right]}{\mathrm{Re}\left[\tilde{T}(x = 0)\right]}\right]. \tag{3.13}$$

In this context, for $n \in \mathbb{N} \cup \{0\}$, we define the following (forward) operators:

$$\widehat{\boldsymbol{F_n}} \colon \left(\mathbb{R}^+\right)^{n+1} \times \mathbb{R} \to \mathbb{R},$$

$$\widehat{\boldsymbol{F_n}}(L_1, \ldots, L_{n+1}; \omega) := \varphi_{\tilde{T}} \tag{3.14}$$

characterizing the $(n + 2)$ layered system.

## 3.2   Modeling of the Inverse Problem

Let us now turn our attention to the derivation of the inverse operators and thus to said inverse problem.

Recall the following (forward) operators:

$$\widehat{F_n} \colon \left(\mathbb{R}^+\right)^{n+1} \times \mathbb{R} \to \mathbb{R},$$

$$\widehat{F_n}(L_1, \ldots, L_{n+1}; \omega) \coloneqq \varphi_{\tilde{T}}$$

derived in Equation (3.14) where $n \in \mathbb{N} \cup \{0\}$. First, for $m \in \mathbb{N}$, expand the operators $F_n$ to the following form:

$$\boldsymbol{F_n} \colon \left(\mathbb{R}^+\right)^{n+1} \times \mathbb{R}^m \to \mathbb{R}^m,$$

$$\boldsymbol{F_n}(L_1, \ldots, L_{n+1}; \omega_1, \ldots, \omega_m) \coloneqq \overline{\varphi_{\tilde{T}}} = \left(\widehat{F_n}(L_1, \ldots, L_{n+1}; \omega_1), \ldots, \widehat{F_n}(L_1, \ldots, L_{n+1}; \omega_m)\right). \tag{3.15}$$

Through this modification, we allow multiple phase images for the same tuple of layer thicknesses differing from each other in terms of the excitation frequency $\omega_i$    , $i = 1, \ldots, m$. This is a crucial step for providing solvability and stability of the problem because more excitation frequencies lead to more data. Thus, as becomes clear in the subsequently performed experiments, this expansion forms an indispensable step.

Assume that measured data $\overline{\varphi_{\tilde{T}_{meas}}} \in \mathbb{R}^m$ is given. To obtain the layer thicknesses $(L_1, \ldots, L_{n+1})$, the idea is to minimize the following expression:

$$||F_n(L_1, \ldots, L_{n+1}; \omega_1, \ldots, \omega_m) - \overline{\varphi_{\tilde{T}_{meas}}}||_2^2.$$

This concept corresponds to a nonlinear least squares approach.

Note that $x_{\min} = \underset{x \in X}{\arg\min} \, f(x) \Leftrightarrow f(x_{min}) = \underset{x \in X}{\min} f(x)$ where $X$ denotes the domain of the function $f$. Then, for fixed excitation frequencies $\omega_1, \ldots \omega_m$ and for given (measured) data $\overline{\varphi_{\tilde{T}_{meas}}} \in \mathbb{R}^m$, we define the following (inverse) operators:

$$\boldsymbol{G_n} \colon \mathbb{R}^m \to \left(\mathbb{R}^+\right)^{n+1},$$

$$\boldsymbol{G_n}(\overline{\varphi_{\tilde{T}_{meas}}}) \coloneqq \underset{(L_1, \ldots, L_{n+1}) \in (\mathbb{R}^+)^{n+1}}{\arg\min} ||F_n(L_1, \ldots, L_{n+1}, \omega_1, \ldots, \omega_m) - \overline{\varphi_{\tilde{T}_{meas}}}||_2^2 \tag{3.16}$$

leading to the inverse problem of *photothermal measurement of layer thicknesses in multilayered systems*.

# 4 Numerical Evaluation

At this point, we want to consider all the theory introduced in the previous section from a more practical point of view. In some short numerical experiments, we test our algorithm (see Section A) that aims to solve the just introduced inverse problem of *photothermal measurement of layer thicknesses in multilayered systems*. The algorithm is programmed in Matlab and relies mainly on the preimplemnted function lsqnonlin. We construct some calculation examples by a variation of the involved parameters. In particular, we distinguish between the number of layers and consider in more detail the two layered, the three layered, and the four layered system. In each one, multiple calculations are performed. Subsequently, we list and discuss the observations.

## 4.1 Experiments

This subsection's object is the performance of several experiments for calculating layer thicknesses by varying and specifying the different quantities that are involved in the algorithm. On the one hand, the goal is to test and validate our code (for details see Section A) providing an overview of upcoming problems. On the other hand, we want to confirm some of the aforementioned facts about thermal waves that come naturally and are introduced in the beginning of this thesis.

Following [17, p. 2948], in each of the further performed experiments we specify the thermophysical properties of the included materials according to the subsequent table:

| Thermal properties of paint samples used in the experiments | | | |
|---|---|---|---|
| Material $M_j, j = 1, \ldots, n$ | Density $\left[\frac{\text{kg}}{\text{m}^3}\right]$ | Thermal conductivity $\left[\frac{\text{W}}{\text{mK}}\right]$ | Specific heat capacity $\left[\frac{\text{J}}{\text{kgK}}\right]$ |
| Paint layer 1 | 1331 | 1.45 | 5184 |
| Paint layer 2 | 1303 | 0.74 | 2557 |
| Paint layer 3 | 1251 | 0.74 | 1670 |
| Paint layer 4 | 1162 | 0.57 | 2835 |
| Substrate layer 1 (aluminum) | 2700 | 238 | 945 |

Table 3: Thermal properties of some paint samples using the photoacoustic scanning technique, see [17, p. 2948] and of pure aluminum, see [12, p. 16]

The main function that we use in our program is lsqnonlin which is preimplemented in Matlab. As input, it receives a function as well as a start value for which the nonlinear least-squares (nonlinear data-fitting) problem of the form:

$$\min_x ||f(x)||_2^2 = \min_x \left( f_1(x)^2 + f_2(x)^2 + \cdots + f_n(x)^2 \right)$$

with optional lower and upper bounds *lb* and *ub* on the components of $x$ is solved by finding a minimum of the sum of squares of the given function.

Subsequently, we present the results of a series of calculation examples beginning with the

two layered system before then continuing with the three layered system and finishing with the four layered system. In each experiment, the substrate layer and the coating layers are chosen according to Table 3. Thus, the substrate layer is the same in each experiment and the coating layers are chosen from the table in ascending order. We consider exact data on the one hand and noisy data on the other hand. For reasons of simplicity, each coating layer possesses the same thickness, namely $5 \times 10^{-5}$ m. In real life applications, this could be a typical value for the thickness of a coating layer. Furthermore, we vary the excitation frequencies $\omega = 2 * \pi * f$. In this context, we chose to start with small values for the quantity $f$, leading to a deeper penetration of the material and thus fewer ambiguities. In particular, we consider a number of starting values for the least squares method, that are the same in each experiment. On the one hand, our results show the reconstructed thicknesses (denoted by $L_{j\text{calculated}}$, $j = 1, \ldots n - 1$). On the other hand, they show the absolute value of the difference of the phase angle of the exact thickness and the calculated thickness, divided by the phase angle of the exact thickness (i.e., the relative error of the phase angle), depending on the excitation frequency (denoted by error$(\omega_j)$, $j = 1, \ldots, m$). The latter provides us with a quantity describing the error.

It should be noted here that there a countless more options to perform such experiments than the subsequently chosen ones.

**Experiment 1**

Consider a two layered system of materials with specified thermophysical properties according to Table 3. Let $L_{1\text{exact}} = 5 \times 10^{-5}$ m be the exact thickness of the first layer. We want to reconstruct this thickness. We set the parameters according to the following cases:

(1.1) We chose 20 start values $L_{1\text{initial}} \in [1 \times 10^{-5}, 9 \times 10^{-5}]$.

    (1.1.1) Let $\omega_1 = 2 * \pi * 2$ Hz be the modulation frequency.

    (1.1.2) Let $\omega_1 = 2 * \pi * 10$ Hz be the modulation frequency.

    (1.1.3) Let $\omega_1 = 2 * \pi * 0.5$ Hz be the modulation frequency.

    (1.1.4) Let $\omega_1 = 2 * \pi * 0.5$ Hz and $\omega_2 = 2 * \pi * 10$ Hz be the modulation frequencies.

(1.2) We chose 20 start values $L_{1\text{initial}} \in [1 \times 10^{-5}, 9 \times 10^{-5}]$. We add noise in the amount of $10000 \times 10^{-5}$ deg. to the phase angle of the exact data.

    (1.2.1) Let $\omega = 2 * \pi * 10$ Hz be the excitation frequency.

    (1.2.2) Let $\omega = 2 * \pi * 10$ Hz, $\omega_2 = 2 * \pi * 0.5$ Hz be the excitation frequencies.

    (1.2.3) Let $\omega = 2 * \pi * 10$ Hz, $\omega_2 = 2 * \pi * 0.5$ Hz, $\omega_3 = 2 * \pi * 2$ Hz be the excitation frequencies.

| $L_{1\text{initial}}$ [m] | $L_{1\text{calculated}}$ [m] | error($\omega_1$) [deg.] |
|---|---|---|
| $1.0000 \times 10^{-5}$ | $4.9994 \times 10^{-5}$ | $0.73697 \times 10^{-5}$ |
| $1.4211 \times 10^{-5}$ | $4.9999 \times 10^{-5}$ | $0.10273 \times 10^{-5}$ |
| $1.8421 \times 10^{-5}$ | $4.9968 \times 10^{-5}$ | $4.1142 \times 10^{-5}$ |
| $2.2632 \times 10^{-5}$ | $4.9993 \times 10^{-5}$ | $0.96053 \times 10^{-5}$ |
| $2.6842 \times 10^{-5}$ | $4.9999 \times 10^{-5}$ | $0.14068 \times 10^{-5}$ |
| $3.1053 \times 10^{-5}$ | $4.9966 \times 10^{-5}$ | $4.3653 \times 10^{-5}$ |
| $3.5263 \times 10^{-5}$ | $4.9994 \times 10^{-5}$ | $0.73245 \times 10^{-5}$ |
| $3.9474 \times 10^{-5}$ | $4.9935 \times 10^{-5}$ | $8.4819 \times 10^{-5}$ |
| $4.3684 \times 10^{-5}$ | $4.9995 \times 10^{-5}$ | $0.67393 \times 10^{-5}$ |
| $4.7895 \times 10^{-5}$ | $4.9992 \times 10^{-5}$ | $1.0291 \times 10^{-5}$ |
| $5.2105 \times 10^{-5}$ | $4.9966 \times 10^{-5}$ | $4.3676 \times 10^{-5}$ |
| $5.6316 \times 10^{-5}$ | $6.2229 \times 10^{-5}$ | $0.08676 \times 10^{-5}$ |
| $6.0526 \times 10^{-5}$ | $6.2234 \times 10^{-5}$ | $0.67434 \times 10^{-5}$ |
| $6.4737 \times 10^{-5}$ | $6.2236 \times 10^{-5}$ | $0.85322 \times 10^{-5}$ |
| $6.8947 \times 10^{-5}$ | $6.223 \times 10^{-5}$ | $0.16798 \times 10^{-5}$ |
| $7.3158 \times 10^{-5}$ | $6.2242 \times 10^{-5}$ | $1.5373 \times 10^{-5}$ |
| $7.7368 \times 10^{-5}$ | $6.2276 \times 10^{-5}$ | $5.4253 \times 10^{-5}$ |
| $8.1579 \times 10^{-5}$ | $6.2229 \times 10^{-5}$ | $0.10676 \times 10^{-5}$ |
| $8.5789 \times 10^{-5}$ | $6.2231 \times 10^{-5}$ | $0.31714 \times 10^{-5}$ |
| $9.0000 \times 10^{-5}$ | $6.2234 \times 10^{-5}$ | $0.72118 \times 10^{-5}$ |

Table 4: Results for case (1.1.1)

| $L_{1\text{initial}}$ [m] | $L_{1\text{calculated}}$ [m] | error($\omega_1$) [deg.] |
|---|---|---|
| $1.0000 \times 10^{-5}$ | $94.924 \times 10^{-5}$ | $0.03421 \times 10^{-5}$ |
| $1.4211 \times 10^{-5}$ | $94.857 \times 10^{-5}$ | $29.775 \times 10^{-5}$ |
| $1.8421 \times 10^{-5}$ | $94.915 \times 10^{-5}$ | $4.3449 \times 10^{-5}$ |
| $2.2632 \times 10^{-5}$ | $94.917 \times 10^{-5}$ | $3.2181 \times 10^{-5}$ |
| $2.6842 \times 10^{-5}$ | $5.0000 \times 10^{-5}$ | $0.51941 \times 10^{-5}$ |
| $3.1053 \times 10^{-5}$ | $5.0000 \times 10^{-5}$ | $0.01117 \times 10^{-5}$ |
| $3.5263 \times 10^{-5}$ | $5.0000 \times 10^{-5}$ | $0.65243 \times 10^{-5}$ |
| $3.9474 \times 10^{-5}$ | $5.0000 \times 10^{-5}$ | $0.02233 \times 10^{-5}$ |
| $4.3684 \times 10^{-5}$ | $5.0003 \times 10^{-5}$ | $4.07772 \times 10^{-5}$ |
| $4.7895 \times 10^{-5}$ | $5.0000 \times 10^{-5}$ | $0.03702 \times 10^{-5}$ |
| $5.2105 \times 10^{-5}$ | $5.0000 \times 10^{-5}$ | $0.02291 \times 10^{-5}$ |
| $5.6316 \times 10^{-5}$ | $5.0000 \times 10^{-5}$ | $0.71521 \times 10^{-5}$ |
| $6.0526 \times 10^{-5}$ | $5.0002 \times 10^{-5}$ | $2.49911 \times 10^{-5}$ |
| $6.4737 \times 10^{-5}$ | $5.0002 \times 10^{-5}$ | $3.4363 \times 10^{-5}$ |
| $6.8947 \times 10^{-5}$ | $5.0001 \times 10^{-5}$ | $1.4903 \times 10^{-5}$ |
| $7.3158 \times 10^{-5}$ | $5.0000 \times 10^{-5}$ | $0.6603 \times 10^{-5}$ |
| $7.7368 \times 10^{-5}$ | $5.0000 \times 10^{-5}$ | $0.06378 \times 10^{-5}$ |
| $8.1579 \times 10^{-5}$ | $5.0000 \times 10^{-5}$ | $0.14089 \times 10^{-5}$ |
| $8.5789 \times 10^{-5}$ | $5.0001 \times 10^{-5}$ | $2.0624 \times 10^{-5}$ |
| $9.0000 \times 10^{-5}$ | $5.0000 \times 10^{-5}$ | $0.00601 \times 10^{-5}$ |

Table 5: Results for case (1.1.2)

| $L_{1\text{initial}}$ [m] | $L_{1\text{calculated}}$ [m] | error($\omega_1$) [deg.] |
|---|---|---|
| $1.0000 \times 10^{-5}$ | $4.9997 \times 10^{-5}$ | $2.0102 \times 10^{-5}$ |
| $1.4211 \times 10^{-5}$ | $4.9999 \times 10^{-5}$ | $0.45565 \times 10^{-5}$ |
| $1.8421 \times 10^{-5}$ | $5.0000 \times 10^{-5}$ | $0.07634 \times 10^{-5}$ |
| $2.2632 \times 10^{-5}$ | $5.0000 \times 10^{-5}$ | $0.007 \times 10^{-5}$ |
| $2.6842 \times 10^{-5}$ | $4.9998 \times 10^{-5}$ | $7.2456 \times 10^{-5}$ |
| $3.1053 \times 10^{-5}$ | $4.9998 \times 10^{-5}$ | $1.6766 \times 10^{-5}$ |
| $3.5263 \times 10^{-5}$ | $5.0000 \times 10^{-5}$ | $0.24801 \times 10^{-5}$ |
| $3.9474 \times 10^{-5}$ | $5.0000 \times 10^{-5}$ | $0.01429 \times 10^{-5}$ |
| $4.3684 \times 10^{-5}$ | $4.9994 \times 10^{-5}$ | $4.2977 \times 10^{-5}$ |
| $4.7895 \times 10^{-5}$ | $5.0000 \times 10^{-5}$ | $0.04651 \times 10^{-5}$ |
| $5.2105 \times 10^{-5}$ | $5.0000 \times 10^{-5}$ | $0.05334 \times 10^{-5}$ |
| $5.6316 \times 10^{-5}$ | $4.9992 \times 10^{-5}$ | $5.7583 \times 10^{-5}$ |
| $6.0526 \times 10^{-5}$ | $5.0000 \times 10^{-5}$ | $0.04441 \times 10^{-5}$ |
| $6.4737 \times 10^{-5}$ | $4.9999 \times 10^{-5}$ | $0.98544 \times 10^{-5}$ |
| $6.8947 \times 10^{-5}$ | $4.9987 \times 10^{-5}$ | $9.5397 \times 10^{-5}$ |
| $7.3158 \times 10^{-5}$ | $5.0000 \times 10^{-5}$ | $0.0695 \times 10^{-5}$ |
| $7.7368 \times 10^{-5}$ | $4.9998 \times 10^{-5}$ | $1.7327 \times 10^{-5}$ |
| $8.1579 \times 10^{-5}$ | $4.9996 \times 10^{-5}$ | $2.7074 \times 10^{-5}$ |
| $8.5789 \times 10^{-5}$ | $4.9997 \times 10^{-5}$ | $2.4424 \times 10^{-5}$ |
| $9.0000 \times 10^{-5}$ | $4.9999 \times 10^{-5}$ | $0.89047 \times 10^{-5}$ |

Table 6: Results for case (1.1.3)

| $L_{1\text{initial}}$ [m] | $L_{1\text{calculated}}$ [m] | error($\omega_1$) [deg.] | error($\omega_2$) [deg.] |
|---|---|---|---|
| $1.0000 \times 10^{-5}$ | $5.0000 \times 10^{-5}$ | $0.00702 \times 10^{-5}$ | $0.01578 \times 10^{-5}$ |
| $1.4211 \times 10^{-5}$ | $5.0001 \times 10^{-5}$ | $0.46868 \times 10^{-5}$ | $1.0531 \times 10^{-5}$ |
| $1.8421 \times 10^{-5}$ | $5.0000 \times 10^{-5}$ | $0.00139 \times 10^{-5}$ | $0.00311 \times 10^{-5}$ |
| $2.2632 \times 10^{-5}$ | $5.0001 \times 10^{-5}$ | $0.50314 \times 10^{-5}$ | $13.0140 \times 10^{-5}$ |
| $1.1306 \times 10^{-5}$ | $5.0000 \times 10^{-5}$ | $0.06685 \times 10^{-5}$ | $0.1502 \times 10^{-5}$ |
| $3.1053 \times 10^{-5}$ | $5.0000 \times 10^{-5}$ | $0.00006 \times 10^{-5}$ | $0.00014 \times 10^{-5}$ |
| $3.5263 \times 10^{-5}$ | $5.0000 \times 10^{-5}$ | $0.1969 \times 10^{-5}$ | $0.26895 \times 10^{-5}$ |
| $3.9474 \times 10^{-5}$ | $5.0001 \times 10^{-5}$ | $0.46739 \times 10^{-5}$ | $1.0502 \times 10^{-5}$ |
| $4.3684 \times 10^{-5}$ | $5.0000 \times 10^{-5}$ | $0.10069 \times 10^{-5}$ | $0.22625 \times 10^{-5}$ |
| $4.7895 \times 10^{-5}$ | $5.0000 \times 10^{-5}$ | $0.00019 \times 10^{-5}$ | $0.0004 \times 10^{-5}$ |
| $5.2105 \times 10^{-5}$ | $5.0000 \times 10^{-5}$ | $0.00016 \times 10^{-5}$ | $0.00035 \times 10^{-5}$ |
| $5.6316 \times 10^{-5}$ | $5.0000 \times 10^{-5}$ | $0.00445 \times 10^{-5}$ | $0.00999 \times 10^{-5}$ |
| $6.0526 \times 10^{-5}$ | $5.0000 \times 10^{-5}$ | $0.14141 \times 10^{-5}$ | $0.31774 \times 10^{-5}$ |
| $6.4737 \times 10^{-5}$ | $5.0000 \times 10^{-5}$ | $0.11508 \times 10^{-5}$ | $0.25858 \times 10^{-5}$ |
| $6.8947 \times 10^{-5}$ | $5.0000 \times 10^{-5}$ | $0.01073 \times 10^{-5}$ | $0.02411 \times 10^{-5}$ |
| $7.3158 \times 10^{-5}$ | $5.0002 \times 10^{-5}$ | $1.4001 \times 10^{-5}$ | $3.14610 \times 10^{-5}$ |
| $7.7368 \times 10^{-5}$ | $5.0000 \times 10^{-5}$ | $0.00019 \times 10^{-5}$ | $0.00027 \times 10^{-5}$ |
| $8.1579 \times 10^{-5}$ | $5.0000 \times 10^{-5}$ | $0.00192 \times 10^{-5}$ | $0.00268 \times 10^{-5}$ |
| $8.5789 \times 10^{-5}$ | $5.0000 \times 10^{-5}$ | $0.00902 \times 10^{-5}$ | $0.20265 \times 10^{-5}$ |
| $9.0000 \times 10^{-5}$ | $5.0001 \times 10^{-5}$ | $0.39794 \times 10^{-5}$ | $0.08942 \times 10^{-5}$ |

Table 7: Results for case (1.1.4)

| $L_{1\text{initial}}$ [m] | $L_{1\text{calculated}}$ [m] | error($\omega_1$) [deg.] |
|---|---|---|
| $1.0000 \times 10^{-5}$ | $0.9587 \times 10^{-5}$ | $411.99004 \times 10^{-5}$ |
| $1.4211 \times 10^{-5}$ | $0.9581 \times 10^{-5}$ | $387.56889 \times 10^{-5}$ |
| $1.8421 \times 10^{-5}$ | $0.9586 \times 10^{-5}$ | $407.67032 \times 10^{-5}$ |
| $2.2632 \times 10^{-5}$ | $0.9587 \times 10^{-5}$ | $410.16189 \times 10^{-5}$ |
| $2.6842 \times 10^{-5}$ | $4.9744 \times 10^{-5}$ | $411.48895 \times 10^{-5}$ |
| $3.1053 \times 10^{-5}$ | $4.9744 \times 10^{-5}$ | $411.97158 \times 10^{-5}$ |
| $3.5263 \times 10^{-5}$ | $4.9745 \times 10^{-5}$ | $411.34038 \times 10^{-5}$ |
| $3.9474 \times 10^{-5}$ | $4.9744 \times 10^{-5}$ | $411.96269 \times 10^{-5}$ |
| $4.3684 \times 10^{-5}$ | $4.9746 \times 10^{-5}$ | $408.40341 \times 10^{-5}$ |
| $4.7895 \times 10^{-5}$ | $4.9744 \times 10^{-5}$ | $411.95899 \times 10^{-5}$ |
| $5.2105 \times 10^{-5}$ | $4.9744 \times 10^{-5}$ | $411.94836 \times 10^{-5}$ |
| $5.6316 \times 10^{-5}$ | $4.9745 \times 10^{-5}$ | $411.11828 \times 10^{-5}$ |
| $6.0526 \times 10^{-5}$ | $4.9746 \times 10^{-5}$ | $409.11571 \times 10^{-5}$ |
| $6.4737 \times 10^{-5}$ | $4.9747 \times 10^{-5}$ | $408.08619 \times 10^{-5}$ |
| $6.8947 \times 10^{-5}$ | $4.9745 \times 10^{-5}$ | $410.22145 \times 10^{-5}$ |
| $7.3158 \times 10^{-5}$ | $4.9745 \times 10^{-5}$ | $411.42744 \times 10^{-5}$ |
| $7.7368 \times 10^{-5}$ | $4.9744 \times 10^{-5}$ | $411.97680 \times 10^{-5}$ |
| $8.1579 \times 10^{-5}$ | $4.9744 \times 10^{-5}$ | $411.83247 \times 10^{-5}$ |
| $8.5789 \times 10^{-5}$ | $4.9746 \times 10^{-5}$ | $409.74028 \times 10^{-5}$ |
| $9.0000 \times 10^{-5}$ | $4.9744 \times 10^{-5}$ | $411.97629 \times 10^{-5}$ |

Table 8: Results for case (1.2.1)

| $L_{1\text{initial}}$ [m] | $L_{1\text{calculated}}$ [m] | error($\omega_1$) [deg.] | error($\omega_2$) [deg.] |
|---|---|---|---|
| $1.0000 \times 10^{-5}$ | $4.9891 \times 10^{-5}$ | $176.15657 \times 10^{-5}$ | $78.613 \times 10^{-5}$ |
| $1.4211 \times 10^{-5}$ | $4.9889 \times 10^{-5}$ | $178.72308 \times 10^{-5}$ | $79.761 \times 10^{-5}$ |
| $1.8421 \times 10^{-5}$ | $4.9891 \times 10^{-5}$ | $175.94378 \times 10^{-5}$ | $78.517 \times 10^{-5}$ |
| $2.2632 \times 10^{-5}$ | $4.9889 \times 10^{-5}$ | $178.90703 \times 10^{-5}$ | $79.843 \times 10^{-5}$ |
| $2.6842 \times 10^{-5}$ | $4.9887 \times 10^{-5}$ | $177.18917 \times 10^{-5}$ | $79.075 \times 10^{-5}$ |
| $3.1053 \times 10^{-5}$ | $4.9891 \times 10^{-5}$ | $175.89658 \times 10^{-5}$ | $78.496 \times 10^{-5}$ |
| $3.5263 \times 10^{-5}$ | $4.9889 \times 10^{-5}$ | $178.31138 \times 10^{-5}$ | $79.577 \times 10^{-5}$ |
| $3.9474 \times 10^{-5}$ | $4.9889 \times 10^{-5}$ | $178.79935 \times 10^{-5}$ | $79.795 \times 10^{-5}$ |
| $4.3684 \times 10^{-5}$ | $4.9890 \times 10^{-5}$ | $177.55137 \times 10^{-5}$ | $79.237 \times 10^{-5}$ |
| $4.7895 \times 10^{-5}$ | $4.9891 \times 10^{-5}$ | $176.05174 \times 10^{-5}$ | $78.566 \times 10^{-5}$ |
| $5.2105 \times 10^{-5}$ | $4.9891 \times 10^{-5}$ | $175.82664 \times 10^{-5}$ | $78.465 \times 10^{-5}$ |
| $5.6316 \times 10^{-5}$ | $4.9891 \times 10^{-5}$ | $176.57316 \times 10^{-5}$ | $78.799 \times 10^{-5}$ |
| $6.0526 \times 10^{-5}$ | $4.9890 \times 10^{-5}$ | $177.22741 \times 10^{-5}$ | $79.092 \times 10^{-5}$ |
| $6.4737 \times 10^{-5}$ | $4.9888 \times 10^{-5}$ | $176.98448 \times 10^{-5}$ | $78.983 \times 10^{-5}$ |
| $6.8947 \times 10^{-5}$ | $4.9892 \times 10^{-5}$ | $174.40701 \times 10^{-5}$ | $77.83 \times 10^{-5}$ |
| $7.3158 \times 10^{-5}$ | $4.9898 \times 10^{-5}$ | $164.23817 \times 10^{-5}$ | $73.28 \times 10^{-5}$ |
| $7.7368 \times 10^{-5}$ | $4.9891 \times 10^{-5}$ | $176.02780 \times 10^{-5}$ | $78.555 \times 10^{-5}$ |
| $8.1579 \times 10^{-5}$ | $4.9891 \times 10^{-5}$ | $176.54156 \times 10^{-5}$ | $78.785 \times 10^{-5}$ |
| $8.5789 \times 10^{-5}$ | $4.9888 \times 10^{-5}$ | $177.57093 \times 10^{-5}$ | $79.245 \times 10^{-5}$ |
| $9.0000 \times 10^{-5}$ | $4.9889 \times 10^{-5}$ | $178.71348 \times 10^{-5}$ | $79.757 \times 10^{-5}$ |

Table 9: Results for case (1.2.2)

| $L_{1\text{initial}}$ [m] | $L_{1\text{calculated}}$ [m] | error($\omega_1$) [deg.] | error($\omega_2$) [deg.] | error($\omega_3$) [deg.] |
|---|---|---|---|---|
| $1.0000 \times 10^{-5}$ | $4.9912 \times 10^{-5}$ | $141.39 \times 10^{-5}$ | $63.064 \times 10^{-5}$ | $11.413 \times 10^{-5}$ |
| $1.4211 \times 10^{-5}$ | $4.9911 \times 10^{-5}$ | $143.17 \times 10^{-5}$ | $63.859 \times 10^{-5}$ | $11.558 \times 10^{-5}$ |
| $1.8421 \times 10^{-5}$ | $4.9912 \times 10^{-5}$ | $142.07 \times 10^{-5}$ | $63.367 \times 10^{-5}$ | $11.468 \times 10^{-5}$ |
| $2.2632 \times 10^{-5}$ | $4.9917 \times 10^{-5}$ | $133.72 \times 10^{-5}$ | $59.637 \times 10^{-5}$ | $10.789 \times 10^{-5}$ |
| $2.6842 \times 10^{-5}$ | $4.9911 \times 10^{-5}$ | $143.64 \times 10^{-5}$ | $64.07 \times 10^{-5}$ | $11.596 \times 10^{-5}$ |
| $3.1053 \times 10^{-5}$ | $4.9912 \times 10^{-5}$ | $142.05 \times 10^{-5}$ | $63.357 \times 10^{-5}$ | $11.466 \times 10^{-5}$ |
| $3.5263 \times 10^{-5}$ | $4.9924 \times 10^{-5}$ | $123.08 \times 10^{-5}$ | $54.882 \times 10^{-5}$ | $9.9236 \times 10^{-5}$ |
| $3.9474 \times 10^{-5}$ | $4.9912 \times 10^{-5}$ | $142.27 \times 10^{-5}$ | $63.458 \times 10^{-5}$ | $11.485 \times 10^{-5}$ |
| $4.3684 \times 10^{-5}$ | $4.9911 \times 10^{-5}$ | $143.31 \times 10^{-5}$ | $63.921 \times 10^{-5}$ | $11.569 \times 10^{-5}$ |
| $4.7895 \times 10^{-5}$ | $4.9912 \times 10^{-5}$ | $141.44 \times 10^{-5}$ | $63.087 \times 10^{-5}$ | $11.417 \times 10^{-5}$ |
| $5.2105 \times 10^{-5}$ | $4.9913 \times 10^{-5}$ | $140.81 \times 10^{-5}$ | $62.805 \times 10^{-5}$ | $11.417 \times 10^{-5}$ |
| $5.6316 \times 10^{-5}$ | $4.9912 \times 10^{-5}$ | $141.97 \times 10^{-5}$ | $63.322 \times 10^{-5}$ | $11.366 \times 10^{-5}$ |
| $6.0526 \times 10^{-5}$ | $4.9911 \times 10^{-5}$ | $143.61 \times 10^{-5}$ | $64.056 \times 10^{-5}$ | $11.46 \times 10^{-5}$ |
| $6.4737 \times 10^{-5}$ | $4.9911 \times 10^{-5}$ | $144.26 \times 10^{-5}$ | $64.348 \times 10^{-5}$ | $11.594 \times 10^{-5}$ |
| $6.8947 \times 10^{-5}$ | $4.9912 \times 10^{-5}$ | $142.57 \times 10^{-5}$ | $63.59 \times 10^{-5}$ | $11.647 \times 10^{-5}$ |
| $7.3158 \times 10^{-5}$ | $4.9916 \times 10^{-5}$ | $136.03 \times 10^{-5}$ | $60.669 \times 10^{-5}$ | $10.977 \times 10^{-5}$ |
| $7.7368 \times 10^{-5}$ | $4.9913 \times 10^{-5}$ | $141.1 \times 10^{-5}$ | $62.936 \times 10^{-5}$ | $11.39 \times 10^{-5}$ |
| $8.1579 \times 10^{-5}$ | $4.9912 \times 10^{-5}$ | $141.148 \times 10^{-5}$ | $63.105 \times 10^{-5}$ | $11.42 \times 10^{-5}$ |
| $8.5789 \times 10^{-5}$ | $4.9912 \times 10^{-5}$ | $142.18 \times 10^{-5}$ | $63.415 \times 10^{-5}$ | $11.477 \times 10^{-5}$ |
| $9.0000 \times 10^{-5}$ | $4.9911 \times 10^{-5}$ | $143.12 \times 10^{-5}$ | $63.834 \times 10^{-5}$ | $11.553 \times 10^{-5}$ |

Table 10: Results for case (1.2.3)

**Experiment 2**

Consider a three layered system of materials with specified thermophysical properties according to Table 3. Let $L_{1\text{exact}} = L_{2\text{exact}} = 5 \times 10^{-5}$ m be the exact thicknesses of the layers. We want to reconstruct both of these thicknesses. We set the parameters according to the following cases:

(2.1) We chose 20 start values $L_{\text{initial}} := L_{1\text{initial}} = L_{2\text{initial}} \in [1 \times 10^{-5}, 9 \times 10^{-5}]$.

  (2.1.1) Let $\omega_1 = 2 * \pi * 10$ Hz be the excitation frequency.

  (2.1.2) Let $\omega_1 = 2 * \pi * 10$ Hz, $\omega_2 = 2 * \pi * 0.5$ Hz be the excitation frequencies.

  (2.1.3) Let $\omega_1 = 2 * \pi * 10$ Hz, $\omega_2 = 2 * \pi * 0.5$ Hz, $\omega_3 = 2 * \pi * 2$ Hz be the excitation frequencies.

(2.2) We chose 20 start values $L_{\text{initial}} := L_{1\text{initial}} = L_{2\text{initial}} \in [1 \times 10^{-5}, 9 \times 10^{-5}]$. Furthermore, we add noise in the amount of $1000 \times 10^{-5}$ deg. to the phase angle of the exact data.

  (2.2.1) Let $\omega_1 = 2 * \pi * 10$ Hz, $\omega_2 = 2 * \pi * 0.5$ Hz be the excitation frequencies.

  (2.2.2) Let $\omega_1 = 2 * \pi * 10$ Hz, $\omega_2 = 2 * \pi * 0.5$ Hz, $\omega_3 = 2 * \pi * 2$ Hz be the excitation frequencies.

| $L_{\text{initial}}$ [m] | $L_{1\text{calculated}}$ [m] | $L_{2\text{calculated}}$ [m] | error($\omega_1$) [deg.] |
|---|---|---|---|
| $1.0000 \times 10^{-5}$ | $17.326 \times 10^{-5}$ | $65.032 \times 10^{-5}$ | $78548 \times 10^{-5}$ |
| $1.4211 \times 10^{-5}$ | $7.3241 \times 10^{-5}$ | $4.8581 \times 10^{-5}$ | $0.000000096105 \times 10^{-5}$ |
| $1.8421 \times 10^{-5}$ | $5.0534 \times 10^{-5}$ | $4.9787 \times 10^{-5}$ | $0.00000014225 \times 10^{-5}$ |
| $2.2632 \times 10^{-5}$ | $4.8032 \times 10^{-5}$ | $5.0848 \times 10^{-5}$ | $0.000000005653 \times 10^{-5}$ |
| $2.6842 \times 10^{-5}$ | $4.7396 \times 10^{-5}$ | $5.1143 \times 10^{-5}$ | $0.000000010711 \times 10^{-5}$ |
| $3.1053 \times 10^{-5}$ | $4.7231 \times 10^{-5}$ | $5.1222 \times 10^{-5}$ | $0.000011049 \times 10^{-5}$ |
| $3.5263 \times 10^{-5}$ | $4.7291 \times 10^{-5}$ | $5.1193 \times 10^{-5}$ | $0.00000051501 \times 10^{-5}$ |
| $3.9474 \times 10^{-5}$ | $4.7551 \times 10^{-5}$ | $5.1070 \times 10^{-5}$ | $0.0000001405 \times 10^{-5}$ |
| $4.3684 \times 10^{-5}$ | $4.8088 \times 10^{-5}$ | $5.0823 \times 10^{-5}$ | $0.000000004959 \times 10^{-5}$ |
| $4.7895 \times 10^{-5}$ | $4.9120 \times 10^{-5}$ | $5.0367 \times 10^{-5}$ | $0.000000053367 \times 10^{-5}$ |
| $5.2105 \times 10^{-5}$ | $5.1355 \times 10^{-5}$ | $4.9474 \times 10^{-5}$ | $0.000000055416 \times 10^{-5}$ |
| $5.6316 \times 10^{-5}$ | $5.6868 \times 10^{-5}$ | $4.7807 \times 10^{-5}$ | $0.0000086754 \times 10^{-5}$ |
| $6.0526 \times 10^{-5}$ | $6.762 \times 10^{-5}$ | $4.7025 \times 10^{-5}$ | $0.00000018136 \times 10^{-5}$ |
| $6.4737 \times 10^{-5}$ | $7.9035 \times 10^{-5}$ | $5.3621 \times 10^{-5}$ | $0.0000000054 \times 10^{-5}$ |
| $6.8947 \times 10^{-5}$ | $8.2654 \times 10^{-5}$ | $6.4008 \times 10^{-5}$ | $0.00000020577 \times 10^{-5}$ |
| $7.3158 \times 10^{-5}$ | $8.3334 \times 10^{-5}$ | $7.1544 \times 10^{-5}$ | $0.000000147860 \times 10^{-5}$ |
| $7.7368 \times 10^{-5}$ | $8.3390 \times 10^{-5}$ | $7.7110 \times 10^{-5}$ | $0.000000177570 \times 10^{-5}$ |
| $8.1579 \times 10^{-5}$ | $8.3264 \times 10^{-5}$ | $8.1627 \times 10^{-5}$ | $0.000000003869 \times 10^{-5}$ |
| $8.5789 \times 10^{-5}$ | $8.3066 \times 10^{-5}$ | $8.5585 \times 10^{-5}$ | $0.000000072356 \times 10^{-5}$ |
| $9.0000 \times 10^{-5}$ | $8.2829 \times 10^{-5}$ | $8.9234 \times 10^{-5}$ | $0.0000000082653 \times 10^{-5}$ |

Table 11: Results for case (2.1.1)

| $L_{\text{initial}}$ [m] | $L_{1\text{calculated}}$ [m] | $L_{2\text{calculated}}$ [m] | error($\omega_1$) [deg.] | error($\omega_2$) [deg.] |
|---|---|---|---|---|
| $1.0000 \times 10^{-5}$ | $18.889 \times 10^{-5}$ | $1.9151 \times 10^{-5}$ | $81858 \times 10^{-5}$ | $6154.2 \times 10^{-5}$ |
| $1.4211 \times 10^{-5}$ | $19.935 \times 10^{-5}$ | $2.1721 \times 10^{-5}$ | $81800 \times 10^{-5}$ | $6977.6 \times 10^{-5}$ |
| $1.8421 \times 10^{-5}$ | $5.0000 \times 10^{-5}$ | $5.0000 \times 10^{-5}$ | $0.0004144 \times 10^{-5}$ | $0.0000035194 \times 10^{-5}$ |
| $2.2632 \times 10^{-5}$ | $4.9998 \times 10^{-5}$ | $4.9999 \times 10^{-5}$ | $7.8595 \times 10^{-5}$ | $0.40571 \times 10^{-5}$ |
| $2.6842 \times 10^{-5}$ | $5.0000 \times 10^{-5}$ | $5.0000 \times 10^{-5}$ | $0.86286 \times 10^{-5}$ | $0.0019868 \times 10^{-5}$ |
| $3.1053 \times 10^{-5}$ | $5.0004 \times 10^{-5}$ | $4.9993 \times 10^{-5}$ | $26.385 \times 10^{-5}$ | $0.46792 \times 10^{-5}$ |
| $3.5263 \times 10^{-5}$ | $5.0000 \times 10^{-5}$ | $5.0000 \times 10^{-5}$ | $0.21036 \times 10^{-5}$ | $0.00076563 \times 10^{-5}$ |
| $3.9474 \times 10^{-5}$ | $5.0004 \times 10^{-5}$ | $4.9994 \times 10^{-5}$ | $18.186 \times 10^{-5}$ | $0.54761 \times 10^{-5}$ |
| $4.3684 \times 10^{-5}$ | $5.0000 \times 10^{-5}$ | $5.0000 \times 10^{-5}$ | $0.99847 \times 10^{-5}$ | $0.0045173 \times 10^{-5}$ |
| $4.7895 \times 10^{-5}$ | $4.9999 \times 10^{-5}$ | $4.9999 \times 10^{-5}$ | $7.8834 \times 10^{-5}$ | $0.3151 \times 10^{-5}$ |
| $5.2105 \times 10^{-5}$ | $4.9998 \times 10^{-5}$ | $4.9999 \times 10^{-5}$ | $8.4717 \times 10^{-5}$ | $0.43143 \times 10^{-5}$ |
| $5.6316 \times 10^{-5}$ | $5.0001 \times 10^{-5}$ | $4.9999 \times 10^{-5}$ | $4.048 \times 10^{-5}$ | $0.0086934 \times 10^{-5}$ |
| $6.0526 \times 10^{-5}$ | $5.0000 \times 10^{-5}$ | $5.0000 \times 10^{-5}$ | $0.0045429 \times 10^{-5}$ | $0.00013484 \times 10^{-5}$ |
| $6.4737 \times 10^{-5}$ | $5.0001 \times 10^{-5}$ | $4.9999 \times 10^{-5}$ | $3.7522 \times 10^{-5}$ | $0.1146 \times 10^{-5}$ |
| $6.8947 \times 10^{-5}$ | $5.0016 \times 10^{-5}$ | $4.9983 \times 10^{-5}$ | $51.25 \times 10^{-5}$ | $2.2189 \times 10^{-5}$ |
| $7.3158 \times 10^{-5}$ | $5.0000 \times 10^{-5}$ | $5.0000 \times 10^{-5}$ | $0.29142 \times 10^{-5}$ | $0.0016838 \times 10^{-5}$ |
| $7.7368 \times 10^{-5}$ | $5.0000 \times 10^{-5}$ | $5.0000 \times 10^{-5}$ | $1.0578 \times 10^{-5}$ | $0.005828 \times 10^{-5}$ |
| $8.1579 \times 10^{-5}$ | $5.0000 \times 10^{-5}$ | $5.0000 \times 10^{-5}$ | $0.86279 \times 10^{-5}$ | $0.0047679 \times 10^{-5}$ |
| $8.5789 \times 10^{-5}$ | $5.0000 \times 10^{-5}$ | $5.0000 \times 10^{-5}$ | $0.10913 \times 10^{-5}$ | $0.00064066 \times 10^{-5}$ |
| $9.0000 \times 10^{-5}$ | $5.0000 \times 10^{-5}$ | $5.0000 \times 10^{-5}$ | $0.0000447 \times 10^{-5}$ | $0.000021508 \times 10^{-5}$ |

Table 12: Results for case (2.1.2)

| $L_{\text{initial}}$ [m] | $L_{1\text{calculated}}$ [m] | $L_{2\text{calculated}}$ [m] | error($\omega_1$) [deg.] | error($\omega_2$) [deg.] | error($\omega_3$) [deg.] |
|---|---|---|---|---|---|
| $1.0000 \times 10^{-5}$ | $15.313 \times 10^{-5}$ | $0.8709 \times 10^{-5}$ | $89708 \times 10^{-5}$ | $4392.6 \times 10^{-5}$ | $6516.1 \times 10^{-5}$ |
| $1.4211 \times 10^{-5}$ | $15.514 \times 10^{-5}$ | $0.9573 \times 10^{-5}$ | $89389 \times 10^{-5}$ | $4413.2 \times 10^{-5}$ | $6814.9 \times 10^{-5}$ |
| $1.8421 \times 10^{-5}$ | $5.0036 \times 10^{-5}$ | $4.9963 \times 10^{-5}$ | $107.26 \times 10^{-5}$ | $4.9368 \times 10^{-5}$ | $0.93148 \times 10^{-5}$ |
| $2.2632 \times 10^{-5}$ | $5.0000 \times 10^{-5}$ | $4.9998 \times 10^{-5}$ | $8.592 \times 10^{-5}$ | $0.13915 \times 10^{-5}$ | $2.5933 \times 10^{-5}$ |
| $2.6842 \times 10^{-5}$ | $15.333 \times 10^{-5}$ | $0.8725 \times 10^{-5}$ | $89530 \times 10^{-5}$ | $4408.8 \times 10^{-5}$ | $6671.3 \times 10^{-5}$ |
| $3.1053 \times 10^{-5}$ | $5.0001 \times 10^{-5}$ | $4.9999 \times 10^{-5}$ | $1.4706 \times 10^{-5}$ | $0.0084895 \times 10^{-5}$ | $0.006817 \times 10^{-5}$ |
| $3.5263 \times 10^{-5}$ | $5.0000 \times 10^{-5}$ | $5.0000 \times 10^{-5}$ | $1.366 \times 10^{-5}$ | $0.0034983 \times 10^{-5}$ | $0.14334 \times 10^{-5}$ |
| $3.9474 \times 10^{-5}$ | $5.0000 \times 10^{-5}$ | $4.9999 \times 10^{-5}$ | $3.8126 \times 10^{-5}$ | $0.090456 \times 10^{-5}$ | $1.286 \times 10^{-5}$ |
| $4.3684 \times 10^{-5}$ | $5.0004 \times 10^{-5}$ | $4.9996 \times 10^{-5}$ | $11.9 \times 10^{-5}$ | $0.62515 \times 10^{-5}$ | $0.260520 \times 10^{-5}$ |
| $4.7895 \times 10^{-5}$ | $4.9999 \times 10^{-5}$ | $4.9997 \times 10^{-5}$ | $15.196 \times 10^{-5}$ | $0.39085 \times 10^{-5}$ | $5.2684 \times 10^{-5}$ |
| $5.2105 \times 10^{-5}$ | $4.9999 \times 10^{-5}$ | $4.9998 \times 10^{-5}$ | $11.24 \times 10^{-5}$ | $0.27744 \times 10^{-5}$ | $3.8418 \times 10^{-5}$ |
| $5.6316 \times 10^{-5}$ | $5.0001 \times 10^{-5}$ | $4.9999 \times 10^{-5}$ | $1.7407 \times 10^{-5}$ | $0.097752 \times 10^{-5}$ | $0.067806 \times 10^{-5}$ |
| $6.0526 \times 10^{-5}$ | $5.0020 \times 10^{-5}$ | $4.9988 \times 10^{-5}$ | $57.898 \times 10^{-5}$ | $2.8208 \times 10^{-5}$ | $0.22968 \times 10^{-5}$ |
| $6.4737 \times 10^{-5}$ | $5.0000 \times 10^{-5}$ | $5.0000 \times 10^{-5}$ | $1.1669 \times 10^{-5}$ | $0.029467 \times 10^{-5}$ | $0.40198 \times 10^{-5}$ |
| $6.8947 \times 10^{-5}$ | $5.0000 \times 10^{-5}$ | $5.0000 \times 10^{-5}$ | $0.0049331 \times 10^{-5}$ | $0.00024409 \times 10^{-5}$ | $0.000037 \times 10^{-5}$ |
| $7.3158 \times 10^{-5}$ | $5.0000 \times 10^{-5}$ | $5.0000 \times 10^{-5}$ | $2.1155 \times 10^{-5}$ | $0.001957 \times 10^{-5}$ | $0.46795 \times 10^{-5}$ |
| $7.7368 \times 10^{-5}$ | $4.9999 \times 10^{-5}$ | $4.9998 \times 10^{-5}$ | $13.515 \times 10^{-5}$ | $0.33982 \times 10^{-5}$ | $4.6487 \times 10^{-5}$ |
| $8.1579 \times 10^{-5}$ | $4.9999 \times 10^{-5}$ | $4.9998 \times 10^{-5}$ | $10.121 \times 10^{-5}$ | $0.24942 \times 10^{-5}$ | $3.4576 \times 10^{-5}$ |
| $8.5789 \times 10^{-5}$ | $5.0040 \times 10^{-5}$ | $4.9959 \times 10^{-5}$ | $120.84 \times 10^{-5}$ | $5.5361 \times 10^{-5}$ | $1.1708 \times 10^{-5}$ |
| $9.0000 \times 10^{-5}$ | $5.0000 \times 10^{-5}$ | $5.0000 \times 10^{-5}$ | $0.31339 \times 10^{-5}$ | $0.0078885 \times 10^{-5}$ | $0.10784 \times 10^{-5}$ |

Table 13: Results for case (2.1.3)

| $L_{\text{initial}}$ [m] | $L_{1\text{calculated}}$ [m] | $L_{2\text{calculated}}$ [m] | error($\omega_1$) [deg.] | error($\omega_2$) [deg.] |
|---|---|---|---|---|
| $1.0000 \times 10^{-5}$ | $18.2690 \times 10^{-5}$ | $1.5276 \times 10^{-5}$ | $80342 \times 10^{-5}$ | $6387.4 \times 10^{-5}$ |
| $1.4211 \times 10^{-5}$ | $19.6470 \times 10^{-5}$ | $2.2730 \times 10^{-5}$ | $83160 \times 10^{-5}$ | $6228.5 \times 10^{-5}$ |
| $1.8421 \times 10^{-5}$ | $4.9822 \times 10^{-5}$ | $5.0035 \times 10^{-5}$ | $184.36 \times 10^{-5}$ | $31.846 \times 10^{-5}$ |
| $2.2632 \times 10^{-5}$ | $4.9820 \times 10^{-5}$ | $5.0037 \times 10^{-5}$ | $176.80 \times 10^{-5}$ | $32.133 \times 10^{-5}$ |
| $2.6842 \times 10^{-5}$ | $4.9821 \times 10^{-5}$ | $5.0037 \times 10^{-5}$ | $174.27 \times 10^{-5}$ | $31.954 \times 10^{-5}$ |
| $3.1053 \times 10^{-5}$ | $4.9825 \times 10^{-5}$ | $5.0031 \times 10^{-5}$ | $196.53 \times 10^{-5}$ | $31.550 \times 10^{-5}$ |
| $3.5263 \times 10^{-5}$ | $4.9821 \times 10^{-5}$ | $5.0037 \times 10^{-5}$ | $173.78 \times 10^{-5}$ | $31.961 \times 10^{-5}$ |
| $3.9474 \times 10^{-5}$ | $4.9825 \times 10^{-5}$ | $5.0032 \times 10^{-5}$ | $191.55 \times 10^{-5}$ | $31.379 \times 10^{-5}$ |
| $4.3684 \times 10^{-5}$ | $4.9821 \times 10^{-5}$ | $5.0037 \times 10^{-5}$ | $174.59 \times 10^{-5}$ | $31.924 \times 10^{-5}$ |
| $4.7895 \times 10^{-5}$ | $4.9819 \times 10^{-5}$ | $5.0037 \times 10^{-5}$ | $180.74 \times 10^{-5}$ | $32.261 \times 10^{-5}$ |
| $5.2105 \times 10^{-5}$ | $4.9819 \times 10^{-5}$ | $5.0036 \times 10^{-5}$ | $183.30 \times 10^{-5}$ | $32.445 \times 10^{-5}$ |
| $5.6316 \times 10^{-5}$ | $4.9822 \times 10^{-5}$ | $5.0036 \times 10^{-5}$ | $178.10 \times 10^{-5}$ | $31.872 \times 10^{-5}$ |
| $6.0526 \times 10^{-5}$ | $4.9821 \times 10^{-5}$ | $5.0038 \times 10^{-5}$ | $173.67 \times 10^{-5}$ | $31.969 \times 10^{-5}$ |
| $6.4737 \times 10^{-5}$ | $4.9822 \times 10^{-5}$ | $5.0036 \times 10^{-5}$ | $177.93 \times 10^{-5}$ | $31.830 \times 10^{-5}$ |
| $6.8947 \times 10^{-5}$ | $4.9840 \times 10^{-5}$ | $5.0018 \times 10^{-5}$ | $232.12 \times 10^{-5}$ | $29.400 \times 10^{-5}$ |
| $7.3158 \times 10^{-5}$ | $4.9821 \times 10^{-5}$ | $5.0038 \times 10^{-5}$ | $174.00 \times 10^{-5}$ | $0.3199 \times 10^{-5}$ |
| $7.7368 \times 10^{-5}$ | $4.9820 \times 10^{-5}$ | $5.0037 \times 10^{-5}$ | $174.98 \times 10^{-5}$ | $32041.0 \times 10^{-5}$ |
| $8.1579 \times 10^{-5}$ | $4.9821 \times 10^{-5}$ | $5.0037 \times 10^{-5}$ | $174.75 \times 10^{-5}$ | $32.029 \times 10^{-5}$ |
| $8.5789 \times 10^{-5}$ | $4.9821 \times 10^{-5}$ | $5.0038 \times 10^{-5}$ | $173.77 \times 10^{-5}$ | $31.976 \times 10^{-5}$ |
| $9.0000 \times 10^{-5}$ | $4.9821 \times 10^{-5}$ | $5.0038 \times 10^{-5}$ | $173.62 \times 10^{-5}$ | $31.967 \times 10^{-5}$ |

Table 14: Results for case (2.2.1)

| $L_{\text{initial}}$ [m] | $L_{1\text{calculated}}$ [m] | $L_{2\text{calculated}}$ [m] | error($\omega_1$) [deg.] | error($\omega_2$) [deg] | error($\omega_3$) [deg.] |
|---|---|---|---|---|---|
| $1.0000 \times 10^{-5}$ | $15.364 \times 10^{-5}$ | $0.8893 \times 10^{-5}$ | $89556 \times 10^{-5}$ | $4404.5 \times 10^{-5}$ | $6650.9 \times 10^{-5}$ |
| $1.4211 \times 10^{-5}$ | $15.507 \times 10^{-5}$ | $0.9561 \times 10^{-5}$ | $89438 \times 10^{-5}$ | $4408.7 \times 10^{-5}$ | $677.12 \times 10^{-5}$ |
| $1.8421 \times 10^{-5}$ | $4.9972 \times 10^{-5}$ | $4.9982 \times 10^{-5}$ | $140.49 \times 10^{-5}$ | $6.1145 \times 10^{-5}$ | $60.467 \times 10^{-5}$ |
| $2.2632 \times 10^{-5}$ | $4.9972 \times 10^{-5}$ | $4.9982 \times 10^{-5}$ | $144.69 \times 10^{-5}$ | $6.144 \times 10^{-5}$ | $61.553 \times 10^{-5}$ |
| $2.6842 \times 10^{-5}$ | $4.9972 \times 10^{-5}$ | $4.9981 \times 10^{-5}$ | $147.33 \times 10^{-5}$ | $6.2588 \times 10^{-5}$ | $62.689 \times 10^{-5}$ |
| $3.1053 \times 10^{-5}$ | $4.9973 \times 10^{-5}$ | $4.9983 \times 10^{-5}$ | $138.33 \times 10^{-5}$ | $5.9791 \times 10^{-5}$ | $59.344 \times 10^{-5}$ |
| $3.5263 \times 10^{-5}$ | $4.9973 \times 10^{-5}$ | $4.9983 \times 10^{-5}$ | $138.2 \times 10^{-5}$ | $6.0187 \times 10^{-5}$ | $59.5 \times 10^{-5}$ |
| $3.9474 \times 10^{-5}$ | $4.9972 \times 10^{-5}$ | $4.9982 \times 10^{-5}$ | $140.7 \times 10^{-5}$ | $6.1164 \times 10^{-5}$ | $60.524 \times 10^{-5}$ |
| $4.3684 \times 10^{-5}$ | $4.9976 \times 10^{-5}$ | $4.9979 \times 10^{-5}$ | $148.12 \times 10^{-5}$ | $5.4839 \times 10^{-5}$ | $59.222 \times 10^{-5}$ |
| $4.7895 \times 10^{-5}$ | $4.9971 \times 10^{-5}$ | $4.9980 \times 10^{-5}$ | $151.84 \times 10^{-5}$ | $6.3748 \times 10^{-5}$ | $64.252 \times 10^{-5}$ |
| $5.2105 \times 10^{-5}$ | $4.9972 \times 10^{-5}$ | $4.9981 \times 10^{-5}$ | $149.14 \times 10^{-5}$ | $6.2986 \times 10^{-5}$ | $63.285 \times 10^{-5}$ |
| $5.6316 \times 10^{-5}$ | $4.9973 \times 10^{-5}$ | $4.9982 \times 10^{-5}$ | $138.67 \times 10^{-5}$ | $5.9637 \times 10^{-5}$ | $59.348 \times 10^{-5}$ |
| $6.0526 \times 10^{-5}$ | $4.9993 \times 10^{-5}$ | $4.9963 \times 10^{-5}$ | $195.25 \times 10^{-5}$ | $3.2602 \times 10^{-5}$ | $59.385 \times 10^{-5}$ |
| $6.4737 \times 10^{-5}$ | $4.9972 \times 10^{-5}$ | $4.9983 \times 10^{-5}$ | $138.26 \times 10^{-5}$ | $6.0695 \times 10^{-5}$ | $59.752 \times 10^{-5}$ |
| $6.8947 \times 10^{-5}$ | $4.9972 \times 10^{-5}$ | $4.9983 \times 10^{-5}$ | $136.98 \times 10^{-5}$ | $6.0519 \times 10^{-5}$ | $59.381 \times 10^{-5}$ |
| $7.3158 \times 10^{-5}$ | $4.9973 \times 10^{-5}$ | $4.9983 \times 10^{-5}$ | $139.37 \times 10^{-5}$ | $6.0455 \times 10^{-5}$ | $59.889 \times 10^{-5}$ |
| $7.7368 \times 10^{-5}$ | $4.9971 \times 10^{-5}$ | $4.9981 \times 10^{-5}$ | $150.67 \times 10^{-5}$ | $6.3466 \times 10^{-5}$ | $63.855 \times 10^{-5}$ |
| $8.1579 \times 10^{-5}$ | $4.9972 \times 10^{-5}$ | $4.9981 \times 10^{-5}$ | $146.96 \times 10^{-5}$ | $6.2567 \times 10^{-5}$ | $62.595 \times 10^{-5}$ |
| $8.5789 \times 10^{-5}$ | $5.0005 \times 10^{-5}$ | $4.9950 \times 10^{-5}$ | $234.24 \times 10^{-5}$ | $1.5302 \times 10^{-5}$ | $60.036 \times 10^{-5}$ |
| $9.0000 \times 10^{-5}$ | $4.9972 \times 10^{-5}$ | $4.9983 \times 10^{-5}$ | $137.3 \times 10^{-5}$ | $6.0521 \times 10^{-5}$ | $59.455 \times 10^{-5}$ |

Table 15: Results for case (2.2.2)

**Experiment 3**

Consider a four layered system of materials with specified thermophysical properties according to Table 3. Let $L_{1\text{exact}} = L_{2\text{exact}} = L_{3\text{exact}} = 5 \times 10^{-5}$ m be the exact thicknesses of the layers. We want to reconstruct all these three thicknesses. We set the parameters according to the following cases:

(3.1) We chose 20 start values $L_{\text{initial}} \coloneqq L_{1\text{initial}} = L_{2\text{initial}} = L_{3\text{initial}} \in [1 \times 10^{-5}, 9 \times 10^{-5}]$.

    (3.1.1) Let $\omega_1 = 2 * \pi * 10$ Hz, $\omega_2 = 2 * \pi * 0.5$ Hz, $\omega_3 = 2 * \pi * 2$ Hz be the excitation frequencies.

    (3.1.2) $\omega_1 = 2 * \pi * 10$ Hz, $\omega_2 = 2 * \pi * 0.5$ Hz, $\omega_3 = 2 * \pi * 2$ Hz, $\omega_4 = 2 * \pi * 20$ Hz be the excitation frequencies.

(3.2) We chose 20 start values $L_{\text{initial}} \coloneqq L_{1\text{initial}} = L_{2\text{initial}} = L_{3\text{initial}} \in [1 \times 10^{-5}, 9 \times 10^{-5}]$. Furthermore, we add noise in the amount of $1000 \times 10^{-5}$ deg. to the phase angle of the exact data.

    (3.2.1) Let $\omega_1 = 2 * \pi * 10$ Hz, $\omega_2 = 2 * \pi * 0.5$ Hz, $\omega_3 = 2 * \pi * 2$ Hz.

    (3.2.2) Let $\omega_1 = 2 * \pi * 10$ Hz, $\omega_2 = 2 * \pi * 0.5$ Hz, $\omega_3 = 2 * \pi * 2$ Hz, $\omega_4 = 2 * \pi * 20$ Hz.

| $L_{\text{initial}}$ [m] | $L_{1\text{calculated}}$ [m] | $L_{2\text{calculated}}$ [m] | $L_{3\text{calculated}}$ [m] | error($\omega_1$) [deg.] | error($\omega_2$) [deg.] | error($\omega_3$) [deg.] |
|---|---|---|---|---|---|---|
| $1.0000 \times 10^{-5}$ | $2.1765 \times 10^{-5}$ | $29.0820 \times 10^{-5}$ | $18.9870 \times 10^{-5}$ | $0.00050208 \times 10^{-5}$ | $0.0079317 \times 10^{-5}$ | $0.018133 \times 10^{-5}$ |
| $1.4211 \times 10^{-5}$ | $0.2544 \times 10^{-5}$ | $91.1770 \times 10^{-5}$ | $128.6800 \times 10^{-5}$ | $79438 \times 10^{-5}$ | $74950 \times 10^{-5}$ | $115730 \times 10^{-5}$ |
| $1.8421 \times 10^{-5}$ | $1.8059 \times 10^{-5}$ | $15.5800 \times 10^{-5}$ | $0.0055 \times 10^{-5}$ | $2312.4 \times 10^{-5}$ | $2455.1 \times 10^{-5}$ | $4034.8 \times 10^{-5}$ |
| $2.2632 \times 10^{-5}$ | $2.1765 \times 10^{-5}$ | $29.0820 \times 10^{-5}$ | $18.9870 \times 10^{-5}$ | $0.0002112 \times 10^{-5}$ | $0.1218 \times 10^{-5}$ | $0.2722 \times 10^{-5}$ |
| $2.6842 \times 10^{-5}$ | $2.1765 \times 10^{-5}$ | $29.0820 \times 10^{-5}$ | $18.9870 \times 10^{-5}$ | $0.000073835 \times 10^{-5}$ | $0.010181 \times 10^{-5}$ | $0.019063 \times 10^{-5}$ |
| $3.1053 \times 10^{-5}$ | $4.1989 \times 10^{-5}$ | $23.6860 \times 10^{-5}$ | $15.2140 \times 10^{-5}$ | $0.004294 \times 10^{-5}$ | $0.18946 \times 10^{-5}$ | $0.98049 \times 10^{-5}$ |
| $3.5263 \times 10^{-5}$ | $4.1989 \times 10^{-5}$ | $23.6860 \times 10^{-5}$ | $15.2130 \times 10^{-5}$ | $0.0063563 \times 10^{-5}$ | $0.10134 \times 10^{-5}$ | $0.52467 \times 10^{-5}$ |
| $3.9474 \times 10^{-5}$ | $5.0000 \times 10^{-5}$ | $5.0000 \times 10^{-5}$ | $5.0000 \times 10^{-5}$ | $0.0047195 \times 10^{-5}$ | $0.00091967 \times 10^{-5}$ | $0.0056922 \times 10^{-5}$ |
| $4.3684 \times 10^{-5}$ | $5.0000 \times 10^{-5}$ | $4.9996 \times 10^{-5}$ | $5.0004 \times 10^{-5}$ | $0.25554 \times 10^{-5}$ | $0.037541 \times 10^{-5}$ | $0.2801 \times 10^{-5}$ |
| $4.7895 \times 10^{-5}$ | $5.0000 \times 10^{-5}$ | $4.9999 \times 10^{-5}$ | $5.0001 \times 10^{-5}$ | $0.078896 \times 10^{-5}$ | $0.014107 \times 10^{-5}$ | $0.10042 \times 10^{-5}$ |
| $5.2105 \times 10^{-5}$ | $5.0000 \times 10^{-5}$ | $5.0000 \times 10^{-5}$ | $5.0000 \times 10^{-5}$ | $0.0014611 \times 10^{-5}$ | $0.00031806 \times 10^{-5}$ | $0.0017126 \times 10^{-5}$ |
| $5.6316 \times 10^{-5}$ | $4.7559 \times 10^{-5}$ | $10.1970 \times 10^{-5}$ | $0.0743 \times 10^{-5}$ | $1.1727 \times 10^{-5}$ | $2.6302 \times 10^{-5}$ | $2.2733 \times 10^{-5}$ |
| $6.0526 \times 10^{-5}$ | $4.7558 \times 10^{-5}$ | $10.2230 \times 10^{-5}$ | $0.0487 \times 10^{-5}$ | $0.26887 \times 10^{-5}$ | $2.5914 \times 10^{-5}$ | $3.9055 \times 10^{-5}$ |
| $6.4737 \times 10^{-5}$ | $4.7554 \times 10^{-5}$ | $10.2930 \times 10^{-5}$ | $0.0206 \times 10^{-5}$ | $5.9359 \times 10^{-5}$ | $3.1895 \times 10^{-5}$ | $2.8618 \times 10^{-5}$ |
| $6.8947 \times 10^{-5}$ | $4.1989 \times 10^{-5}$ | $23.6860 \times 10^{-5}$ | $15.2130 \times 10^{-5}$ | $0.080108 \times 10^{-5}$ | $0.011446 \times 10^{-5}$ | $0.1176 \times 10^{-5}$ |
| $7.3158 \times 10^{-5}$ | $4.1989 \times 10^{-5}$ | $23.6860 \times 10^{-5}$ | $15.2130 \times 10^{-5}$ | $0.088008 \times 10^{-5}$ | $0.010751 \times 10^{-5}$ | $0.12174 \times 10^{-5}$ |
| $7.7368 \times 10^{-5}$ | $4.1989 \times 10^{-5}$ | $23.6860 \times 10^{-5}$ | $15.2140 \times 10^{-5}$ | $0.019086 \times 10^{-5}$ | $0.22809 \times 10^{-5}$ | $1.1979 \times 10^{-5}$ |
| $8.1579 \times 10^{-5}$ | $4.1989 \times 10^{-5}$ | $23.6860 \times 10^{-5}$ | $15.2130 \times 10^{-5}$ | $0.0033421 \times 10^{-5}$ | $0.067143 \times 10^{-5}$ | $0.34424 \times 10^{-5}$ |
| $8.5789 \times 10^{-5}$ | $4.1989 \times 10^{-5}$ | $23.6870 \times 10^{-5}$ | $15.2140 \times 10^{-5}$ | $0.087728 \times 10^{-5}$ | $0.83292 \times 10^{-5}$ | $4.4243 \times 10^{-5}$ |
| $9.0000 \times 10^{-5}$ | $4.1989 \times 10^{-5}$ | $23.6870 \times 10^{-5}$ | $15.2150 \times 10^{-5}$ | $0.11155 \times 10^{-5}$ | $1.0326 \times 10^{-5}$ | $5.489 \times 10^{-5}$ |

Table 16: Results for case (3.1.1)

| $L_{\text{initial}}$ [m] | $L_{1\text{calculated}}$ [m] | $L_{2\text{calculated}}$ [m] | $L_{3\text{calculated}}$ [m] | error($\omega_1$) [deg.] | error($\omega_2$) [deg.] | error($\omega_3$) [deg.] | error($\omega_4$) [deg.] |
|---|---|---|---|---|---|---|---|
| $1.0000 \times 10^{-5}$ | $1.2452 \times 10^{-5}$ | $32.504 \times 10^{-5}$ | $20.668 \times 10^{-5}$ | $23795 \times 10^{-5}$ | $18.049 \times 10^{-5}$ | $2676.6 \times 10^{-5}$ | $46019 \times 10^{-5}$ |
| $1.4211 \times 10^{-5}$ | $1.2457 \times 10^{-5}$ | $32.502 \times 10^{-5}$ | $20.669 \times 10^{-5}$ | $23776 \times 10^{-5}$ | $19.956 \times 10^{-5}$ | $2679.3 \times 10^{-5}$ | $46046 \times 10^{-5}$ |
| $1.8421 \times 10^{-5}$ | $0.7271 \times 10^{-5}$ | $5.7177 \times 10^{-5}$ | $14.2660 \times 10^{-5}$ | $16407 \times 10^{-5}$ | $4057.1 \times 10^{-5}$ | $6143.2 \times 10^{-5}$ | $23466 \times 10^{-5}$ |
| $2.2632 \times 10^{-5}$ | $5.0000 \times 10^{-5}$ | $5.0000 \times 10^{-5}$ | $5.0000 \times 10^{-5}$ | $0.0003327 \times 10^{-5}$ | $0.000020906$ | $0.000044349 \times 10^{-5}$ | $0.000028469 \times 10^{-5}$ |
| $2.6842 \times 10^{-5}$ | $4.8862 \times 10^{-5}$ | $10.8660 \times 10^{-5}$ | $0.7625 \times 10^{-5}$ | $1762 \times 10^{-5}$ | $160.09 \times 10^{-5}$ | $112.65 \times 10^{-5}$ | $1815.3 \times 10^{-5}$ |
| $3.1053 \times 10^{-5}$ | $5.0000 \times 10^{-5}$ | $5.0000 \times 10^{-5}$ | $5.0000 \times 10^{-5}$ | $0.0009042 \times 10^{-5}$ | $0.000010214 \times 10^{-5}$ | $0.00047513 \times 10^{-5}$ | $0.00055375 \times 10^{-5}$ |
| $3.5263 \times 10^{-5}$ | $5.0000 \times 10^{-5}$ | $4.9999 \times 10^{-5}$ | $5.0001 \times 10^{-5}$ | $0.22824 \times 10^{-5}$ | $0.039083 \times 10^{-5}$ | $0.23501 \times 10^{-5}$ | $0.42848 \times 10^{-5}$ |
| $3.9474 \times 10^{-5}$ | $4.8838 \times 10^{-5}$ | $10.969 \times 10^{-5}$ | $0.8608 \times 10^{-5}$ | $1727.7 \times 10^{-5}$ | $160.52 \times 10^{-5}$ | $161.95 \times 10^{-5}$ | $1893.1 \times 10^{-5}$ |
| $4.3684 \times 10^{-5}$ | $5.0000 \times 10^{-5}$ | $5.0000 \times 10^{-5}$ | $5.0000 \times 10^{-5}$ | $0.015257 \times 10^{-5}$ | $0.0025732 \times 10^{-5}$ | $0.015753 \times 10^{-5}$ | $0.023564 \times 10^{-5}$ |
| $4.7895 \times 10^{-5}$ | $5.0000 \times 10^{-5}$ | $4.9999 \times 10^{-5}$ | $5.0001 \times 10^{-5}$ | $0.29193 \times 10^{-5}$ | $0.051253 \times 10^{-5}$ | $0.31316 \times 10^{-5}$ | $0.56483 \times 10^{-5}$ |
| $5.2105 \times 10^{-5}$ | $5.0000 \times 10^{-5}$ | $5.0000 \times 10^{-5}$ | $5.0000 \times 10^{-5}$ | $0.11358 \times 10^{-5}$ | $0.019269 \times 10^{-5}$ | $0.11554 \times 10^{-5}$ | $0.20687 \times 10^{-5}$ |
| $5.6316 \times 10^{-5}$ | $5.0000 \times 10^{-5}$ | $5.0000 \times 10^{-5}$ | $5.0000 \times 10^{-5}$ | $0.0015814 \times 10^{-5}$ | $0.000065258 \times 10^{-5}$ | $0.00036274 \times 10^{-5}$ | $0.0003078 \times 10^{-5}$ |
| $6.0526 \times 10^{-5}$ | $5.0000 \times 10^{-5}$ | $5.0000 \times 10^{-5}$ | $5.0000 \times 10^{-5}$ | $0.017557 \times 10^{-5}$ | $0.0029629 \times 10^{-5}$ | $0.018093 \times 10^{-5}$ | $0.027688 \times 10^{-5}$ |
| $6.4737 \times 10^{-5}$ | $5.0000 \times 10^{-5}$ | $5.0000 \times 10^{-5}$ | $5.0000 \times 10^{-5}$ | $0.011811 \times 10^{-5}$ | $0.0017528 \times 10^{-5}$ | $0.0097826 \times 10^{-5}$ | $0.015419 \times 10^{-5}$ |
| $6.8947 \times 10^{-5}$ | $5.0000 \times 10^{-5}$ | $5.0000 \times 10^{-5}$ | $5.0000 \times 10^{-5}$ | $0.012528 \times 10^{-5}$ | $0.0019049 \times 10^{-5}$ | $0.010834 \times 10^{-5}$ | $0.016934$ |
| $7.3158 \times 10^{-5}$ | $5.0000 \times 10^{-5}$ | $5.0000 \times 10^{-5}$ | $5.0000 \times 10^{-5}$ | $0.0032699 \times 10^{-5}$ | $0.00025737 \times 10^{-5}$ | $0.00045282 \times 10^{-5}$ | $0.001138 \times 10^{-5}$ |
| $7.7368 \times 10^{-5}$ | $5.0000 \times 10^{-5}$ | $5.0000 \times 10^{-5}$ | $5.0000 \times 10^{-5}$ | $0.0012986 \times 10^{-5}$ | $0.000021997 \times 10^{-5}$ | $0.0011665 \times 10^{-5}$ | $0.000026051 \times 10^{-5}$ |
| $8.1579 \times 10^{-5}$ | $5.0000 \times 10^{-5}$ | $5.0000 \times 10^{-5}$ | $5.0000 \times 10^{-5}$ | $0.0003762 \times 10^{-5}$ | $0.000022383 \times 10^{-5}$ | $0.00048319 \times 10^{-5}$ | $0.00036627 \times 10^{-5}$ |
| $8.5789 \times 10^{-5}$ | $4.8842 \times 10^{-5}$ | $11.104 \times 10^{-5}$ | $0.9958 \times 10^{-5}$ | $1733 \times 10^{-5}$ | $163.23 \times 10^{-5}$ | $205.96 \times 10^{-5}$ | $1871.2 \times 10^{-5}$ |
| $9.0000 \times 10^{-5}$ | $1.2467 \times 10^{-5}$ | $32.497 \times 10^{-5}$ | $20.6720 \times 10^{-5}$ | $23737 \times 10^{-5}$ | $28.178 \times 10^{-5}$ | $2694.5 \times 10^{-5}$ | $46098 \times 10^{-5}$ |

Table 17: Results for case (3.1.2)

| $L_{\text{initial}}$ [m] | $L_{1\text{calculated}}$ [m] | $L_{2\text{calculated}}$ [m] | $L_{3\text{calculated}}$ [m] | error($\omega_1$) [deg.] | error($\omega_2$) [deg.] | error($\omega_3$) [deg.] |
|---|---|---|---|---|---|---|
| $1.0000 \times 10^{-5}$ | $2.1708 \times 10^{-5}$ | $2909 \times 10^{-5}$ | $18.978 \times 10^{-5}$ | $82.21 \times 10^{-5}$ | $35.074 \times 10^{-5}$ | $136.73 \times 10^{-5}$ |
| $1.4211 \times 10^{-5}$ | $0.2533 \times 10^{-5}$ | $91.172 \times 10^{-5}$ | $128.67 \times 10^{-5}$ | $79516 \times 10^{-5}$ | $74932 \times 10^{-5}$ | $115670 \times 10^{-5}$ |
| $1.8421 \times 10^{-5}$ | $1.8021 \times 10^{-5}$ | $15.925 \times 10^{-5}$ | $0.0465 \times 10^{-5}$ | $149.81 \times 10^{-5}$ | $2474.3 \times 10^{-5}$ | $3868.2 \times 10^{-5}$ |
| $2.2632 \times 10^{-5}$ | $2.1708 \times 10^{-5}$ | $29.09 \times 10^{-5}$ | $18.978 \times 10^{-5}$ | $82.211 \times 10^{-5}$ | $34.955 \times 10^{-5}$ | $136.47 \times 10^{-5}$ |
| $2.6842 \times 10^{-5}$ | $2.1708 \times 10^{-5}$ | $29.09 \times 10^{-5}$ | $18.978 \times 10^{-5}$ | $82.21 \times 10^{-5}$ | $35.072 \times 10^{-5}$ | $136.730 \times 10^{-5}$ |
| $3.1053 \times 10^{-5}$ | $4.2069 \times 10^{-5}$ | $23.642 \times 10^{-5}$ | $15.144 \times 10^{-5}$ | $82.198 \times 10^{-5}$ | $34.807 \times 10^{-5}$ | $135.3 \times 10^{-5}$ |
| $3.5263 \times 10^{-5}$ | $4.2069 \times 10^{-5}$ | $23.642 \times 10^{-5}$ | $15.144 \times 10^{-5}$ | $82.199 \times 10^{-5}$ | $34.930 \times 10^{-5}$ | $135.94 \times 10^{-5}$ |
| $3.9474 \times 10^{-5}$ | $4.8221 \times 10^{-5}$ | $7.0851 \times 10^{-5}$ | $3.1014 \times 10^{-5}$ | $0.7012 \times 10^{-5}$ | $31.315 \times 10^{-5}$ | $104.1 \times 10^{-5}$ |
| $4.3684 \times 10^{-5}$ | $4.8258 \times 10^{-5}$ | $7.1007 \times 10^{-5}$ | $3.0797 \times 10^{-5}$ | $69.356 \times 10^{-5}$ | $28.624 \times 10^{-5}$ | $141.08 \times 10^{-5}$ |
| $4.7895 \times 10^{-5}$ | $4.8238 \times 10^{-5}$ | $7.1052 \times 10^{-5}$ | $3.0777 \times 10^{-5}$ | $43.568 \times 10^{-5}$ | $31.503 \times 10^{-5}$ | $147.53 \times 10^{-5}$ |
| $5.2105 \times 10^{-5}$ | $4.8317 \times 10^{-5}$ | $7.0014 \times 10^{-5}$ | $3.172 \times 10^{-5}$ | $75.047 \times 10^{-5}$ | $28.702 \times 10^{-5}$ | $147.08 \times 10^{-5}$ |
| $5.6316 \times 10^{-5}$ | $4.7564 \times 10^{-5}$ | $12.1260 \times 10^{-5}$ | $1.8606 \times 10^{-5}$ | $82.218 \times 10^{-5}$ | $35.081 \times 10^{-5}$ | $136.76 \times 10^{-5}$ |
| $6.0526 \times 10^{-5}$ | $4.7564 \times 10^{-5}$ | $12.126 \times 10^{-5}$ | $1.8606 \times 10^{-5}$ | $82.246 \times 10^{-5}$ | $35.077 \times 10^{-5}$ | $136.77 \times 10^{-5}$ |
| $6.4737 \times 10^{-5}$ | $4.7564 \times 10^{-5}$ | $12.126 \times 10^{-5}$ | $1.8606 \times 10^{-5}$ | $82.231 \times 10^{-5}$ | $35.079 \times 10^{-5}$ | $136.76 \times 10^{-5}$ |
| $6.8947 \times 10^{-5}$ | $4.2069 \times 10^{-5}$ | $23.642 \times 10^{-5}$ | $15.144 \times 10^{-5}$ | $82.211 \times 10^{-5}$ | $35.060 \times 10^{-5}$ | $136.64 \times 10^{-5}$ |
| $7.3158 \times 10^{-5}$ | $4.2069 \times 10^{-5}$ | $23.642 \times 10^{-5}$ | $15.144 \times 10^{-5}$ | $82.298 \times 10^{-5}$ | $35.092 \times 10^{-5}$ | $136.87 \times 10^{-5}$ |
| $7.7368 \times 10^{-5}$ | $4.2069 \times 10^{-5}$ | $23.642 \times 10^{-5}$ | $15.144 \times 10^{-5}$ | $82.186 \times 10^{-5}$ | $34.802 \times 10^{-5}$ | $135.25 \times 10^{-5}$ |
| $8.1579 \times 10^{-5}$ | $4.2069 \times 10^{-5}$ | $23.6420 \times 10^{-5}$ | $15.144 \times 10^{-5}$ | $82.206 \times 10^{-5}$ | $34.994 \times 10^{-5}$ | $136.29 \times 10^{-5}$ |
| $8.5789 \times 10^{-5}$ | $4.2069 \times 10^{-5}$ | $23.642 \times 10^{-5}$ | $15.145 \times 10^{-5}$ | $82.096 \times 10^{-5}$ | $34.042 \times 10^{-5}$ | $131.13 \times 10^{-5}$ |
| $9.0000 \times 10^{-5}$ | $4.2069 \times 10^{-5}$ | $23.643 \times 10^{-5}$ | $15.145 \times 10^{-5}$ | $82.07 \times 10^{-5}$ | $33.837 \times 10^{-5}$ | $130.02 \times 10^{-5}$ |

Table 18: Results for case (3.2.1)

| $L_{\text{initial}}$ [m] | $L_{\text{1calculated}}$ [m] | $L_{\text{2calculated}}$ [m] | $L_{\text{3calculated}}$ [m] | error($\omega_1$) [deg.] | error($\omega_2$) [deg.] | error($\omega_3$) [deg.] | error($\omega_4$) [deg.] |
|---|---|---|---|---|---|---|---|
| $1.0000 \times 10^{-5}$ | $1.2421 \times 10^{-5}$ | $32.507 \times 10^{-5}$ | $20.656 \times 10^{-5}$ | $23910 \times 10^{-5}$ | $17.976 \times 10^{-5}$ | $281.27 \times 10^{-5}$ | $45853 \times 10^{-5}$ |
| $1.4211 \times 10^{-5}$ | $1.2426 \times 10^{-5}$ | $32.504 \times 10^{-5}$ | $20.656 \times 10^{-5}$ | $23890 \times 10^{-5}$ | $16.022 \times 10^{-5}$ | $2815.4 \times 10^{-5}$ | $4588 \times 10^{-5}$ |
| $1.8421 \times 10^{-5}$ | $0.7239 \times 10^{-5}$ | $5.7051 \times 10^{-5}$ | $14.288 \times 10^{-5}$ | $16497 \times 10^{-5}$ | $4076.6 \times 10^{-5}$ | $6001.3 \times 10^{-5}$ | $23284 \times 10^{-5}$ |
| $2.2632 \times 10^{-5}$ | $4.8885 \times 10^{-5}$ | $11.067 \times 10^{-5}$ | $0.9691 \times 10^{-5}$ | $1800.5 \times 10^{-5}$ | $153.42 \times 10^{-5}$ | $32.199 \times 10^{-5}$ | $1734.9 \times 10^{-5}$ |
| $2.6842 \times 10^{-5}$ | $5.0042 \times 10^{-5}$ | $4.9945 \times 10^{-5}$ | $4.9952 \times 10^{-5}$ | $73.31 \times 10^{-5}$ | $9.527 \times 10^{-5}$ | $171.38 \times 10^{-5}$ | $131.41 \times 10^{-5}$ |
| $3.1053 \times 10^{-5}$ | $5.0042 \times 10^{-5}$ | $4.9945 \times 10^{-5}$ | $4.9952 \times 10^{-5}$ | $73.312 \times 10^{-5}$ | $9.5268 \times 10^{-5}$ | $171.38 \times 10^{-5}$ | $131.4 \times 10^{-5}$ |
| $3.5263 \times 10^{-5}$ | $5.0042 \times 10^{-5}$ | $4.9944 \times 10^{-5}$ | $4.9953 \times 10^{-5}$ | $73.069 \times 10^{-5}$ | $9.5642 \times 10^{-5}$ | $171.6 \times 10^{-5}$ | $131.07 \times 10^{-5}$ |
| $3.9474 \times 10^{-5}$ | $5.0042 \times 10^{-5}$ | $4.9945 \times 10^{-5}$ | $4.9952 \times 10^{-5}$ | $73.312 \times 10^{-5}$ | $9.5275 \times 10^{-5}$ | $171.39 \times 10^{-5}$ | $131.37 \times 10^{-5}$ |
| $4.3684 \times 10^{-5}$ | $5.0042 \times 10^{-5}$ | $4.9945 \times 10^{-5}$ | $4.9952 \times 10^{-5}$ | $73.312 \times 10^{-5}$ | $9.5274 \times 10^{-5}$ | $171.39 \times 10^{-5}$ | $131.38 \times 10^{-5}$ |
| $4.7895 \times 10^{-5}$ | $5.0042 \times 10^{-5}$ | $4.9945 \times 10^{-5}$ | $4.9952 \times 10^{-5}$ | $73.059 \times 10^{-5}$ | $9.5761 \times 10^{-5}$ | $171.69 \times 10^{-5}$ | $130.73 \times 10^{-5}$ |
| $5.2105 \times 10^{-5}$ | $5.0042 \times 10^{-5}$ | $4.9945 \times 10^{-5}$ | $4.9952 \times 10^{-5}$ | $73.223 \times 10^{-5}$ | $9.5449 \times 10^{-5}$ | $171.5 \times 10^{-5}$ | $131.13 \times 10^{-5}$ |
| $5.6316 \times 10^{-5}$ | $5.0042 \times 10^{-5}$ | $4.9945 \times 10^{-5}$ | $4.9952 \times 10^{-5}$ | $73.311 \times 10^{-5}$ | $9.5269 \times 10^{-5}$ | $171.38 \times 10^{-5}$ | $131.4 \times 10^{-5}$ |
| $6.0526 \times 10^{-5}$ | $5.0042 \times 10^{-5}$ | $4.9945 \times 10^{-5}$ | $4.9952 \times 10^{-5}$ | $73.311 \times 10^{-5}$ | $9.5279 \times 10^{-5}$ | $171.39 \times 10^{-5}$ | $131.37 \times 10^{-5}$ |
| $6.4737 \times 10^{-5}$ | $5.0042 \times 10^{-5}$ | $4.9945 \times 10^{-5}$ | $4.9952 \times 10^{-5}$ | $73.311 \times 10^{-5}$ | $9.5277 \times 10^{-5}$ | $171.39 \times 10^{-5}$ | $131.37 \times 10^{-5}$ |
| $6.8947 \times 10^{-5}$ | $4.8884 \times 10^{-5}$ | $10.9899 \times 10^{-5}$ | $0.8822 \times 10^{-5}$ | $1798.4 \times 10^{-5}$ | $153.73 \times 10^{-5}$ | $24.753 \times 10^{-5}$ | $1740.7 \times 10^{-5}$ |
| $7.3158 \times 10^{-5}$ | $5.004 \times 10^{-5}$ | $4.9961 \times 10^{-5}$ | $4.9936 \times 10^{-5}$ | $74.297 \times 10^{-5}$ | $9.7969 \times 10^{-5}$ | $174.84 \times 10^{-5}$ | $128.58 \times 10^{-5}$ |
| $7.7368 \times 10^{-5}$ | $4.8885 \times 10^{-5}$ | $11.062 \times 10^{-5}$ | $0.9636 \times 10^{-5}$ | $1800.1 \times 10^{-5}$ | $153.49 \times 10^{-5}$ | $32.555 \times 10^{-5}$ | $1735.8 \times 10^{-5}$ |
| $8.1579 \times 10^{-5}$ | $5.0042 \times 10^{-5}$ | $4.9945 \times 10^{-5}$ | $4.9952 \times 10^{-5}$ | $73.312 \times 10^{-5}$ | $9.5275 \times 10^{-5}$ | $171.39 \times 10^{-5}$ | $131.38 \times 10^{-5}$ |
| $8.5789 \times 10^{-5}$ | $5.0042 \times 10^{-5}$ | $4.9945 \times 10^{-5}$ | $4.9952 \times 10^{-5}$ | $73.308 \times 10^{-5}$ | $9.5268 \times 10^{-5}$ | $171.38 \times 10^{-5}$ | $131.4 \times 10^{-5}$ |
| $9.0000 \times 10^{-5}$ | $1.2436 \times 10^{-5}$ | $32.500 \times 10^{-5}$ | $20.6600 \times 10^{-5}$ | $2385.2 \times 10^{-5}$ | $7.618 \times 10^{-5}$ | $2831 \times 10^{-5}$ | $45932 \times 10^{-5}$ |

Table 19: Results for case (3.2.2)

## 4.2 Observations

By observing the previously established calculation tables, we obtain some impressive findings. At this point, we want to discuss them. Notwithstanding the number of chosen layers, we make similar observations in each experiment.

Firstly, when dealing with exact data, we see that, in general, via multiple initial values, we obtain results for the thickness that are near the searched values in the case that the number of excitation frequencies is as big as the number of searched layer thicknesses. Nevertheless, there also occur values that are further away from the aimed solution in this case. When considering the level error, it turns out that there occur non-expedient values for the thicknesses that provide very small errors, leading to ambiguities in the process. Thus, it is generally not possible to find the exact thicknesses. This problem is intensified by increasing the number of layers, as is observable by comparing Table 4 with Table 11. In this context, we observe a strong dependency on the choice of the excitation frequency. For example, comparing Table 4 and Table 5, we find that the former possesses a string of well fitting, but distant values for the thickness, where the latter includes multiple times the exact value of the thickness with relatively small errors. Both tables however consist of ambiguous values that are relatively far away from the exact data. This is not the case for Table 6 where the excitation frequency is chosen the smallest. This is however valid since from the theoretical part of this thesis, we know that in lock-in thermography, we control the reach of the waves into the material by the excitation frequency (in form of the thermal diffusion length $\mu$). We know that small frequencies lead to deeper penetration of the material (since the wave lengths are bigger), providing us with less ambiguity. Furthermore, by comparing the errors, one is able to exclude the non-fitting errors.

Moreover, we observe that by increasing the number of excitation frequencies, we could solve the aforementioned problem of ambiguity. For example, in Table 7, exciting

with two different frequencies, we obtain well fitting values for the thickness via each initial value. Furthermore, the level of error is in general the smallest when dealing with the exact value for the calculated thickness. Similar observations are done in the three and the four layered systems, when considering exact data. For example, when comparing Table 12 and Table 13, there is to be observed that in both cases for multiple initial values, we obtain exact values for the calculated thicknesses with relatively small errors that are getting smaller in Table 13. There are also values that differ crucially from the exact values. However, by observing the level of error, they can be excluded. Table 16 and Table 17 provide similar findings. To increase the number of excitation frequencies is valid because this plan leads to more data and thus solves the problem.

We further see that this step is inevitable when dealing with noisy data. The reason for that is that, of course, inverse problems are generally ill-posed, which is also the case for the inverse problem of the *photothermal measurement of layer thicknesses in multilayered systems*. Thus, small errors in the data lead to big discrepancy in the solutions. One idea to regularize, is simply to increase the number of data which is what we do here. Of course, there are innumerable many approaches to solve the problem. We will address some of them later in Section 5.

Recapitulating, we note that we deal with a sensitive problem. We obtain good results when working with exact data and worse results, leading, without limitation, to ambiguities when working with noisy data without any regularization. This is typical when dealing with inverse problems. We further observe that the adaption and number of excitation frequencies provide a helpful tool to improve the solvability of said problems.

# 5 Conclusion and Outlook

Last but not least, we summarize the most important attainments from the previous sections, as well as give an outlook to further opportunities utilizing the theory of photothermal science. In addition, we briefly address broader problems arising in the practical application of the theory of the photothermal measurement processes. In this context, we take a closer look at possibilities to perform changes in the choice of the parameters in the experiments to obtain different and more impressive results.

In the first place, this thesis dealt with the mathematics and physics of photothermal science, as well as the field's applications. Particularly, we observed the inverse problem of the *photothermal measurement of layer thicknesses in multilayered systems.* In the first part of this thesis (including Sections 1.2 and 2), utilizing the mathematics of heat flow in materials, we derived the basic principles of infrared thermography as well as the foundation of photothermal science. In this context, the lock-in excitation principle defined the chosen technique in this thesis. We found that the thermal diffusion length:

$$\mu = \sqrt{\frac{2\alpha}{\omega}},$$

dependent on the excitation frequency $\omega$ as well as the material's property, is the most crucial quantity when it comes to the *photothermal measurement of layer thicknesses in multilayered systems.* Via this value, we are in the position of specifying the reach of the thermal waves into the material. Employing these findings, we were able to establish the surface temperature of a system of layers of different materials in the second part of this thesis. Via this quantity, we further managed to define the forward problem, consisting in the calculation of the surface temperature's phase angle. We found the following forward operators characterizing said problem (for a $n + 2$ layered system):

$$F_n \colon \left(\mathbb{R}^+\right)^{n+1} \times \mathbb{R}^m \to \mathbb{R}^m,$$

$$F_n(L_1, \ldots, L_{n+1}; \omega_1, \ldots, \omega_m) \coloneqq \overline{\varphi_{\tilde{T}}}$$

After finally introducing the inverse problem of *photothermal measurement of layer thicknesses in multilayered systems* in Section 3 solving:

$$G_n \colon \mathbb{R}^m \to \left(\mathbb{R}^+\right)^{n+1},$$

$$G_n(\overline{\varphi_{\tilde{T}_{meas}}}) \coloneqq \underset{(L_1, \ldots, L_{n+1}) \in (\mathbb{R}^+)^{n+1}}{\arg\min} ||F_n(L_1, \ldots, L_{n+1}, \omega_1, \ldots, \omega_m) - \overline{\varphi_{\tilde{T}_{meas}}}||_2^2,$$

we were able to demonstrate the aforementioned claim about the thermal diffusion length in numerous experiments. These experiments further pointed out the ill-posedness of the treated inverse problem. By varying the number of excitation frequencies in the calculation process, we tried to handle this problem. This proved to be a satisfying approach. Nevertheless, there could be other approaches, one could pursue. We want to

discuss them in detail.

One idea that is common is to introduce a penalty term. In this context, one could vary the considered norm. Another approach is to firstly search for more fitting excitation frequencies. In this thesis, the applied excitation frequencies are more or less chosen with sense of proportion. Of course, one could optimize this selection procedure. Last but not least, instead of performing a nonlinear least-squares approach, one can also use a different method like for example a nonlinear Newton-method. However, there are countless more options to write an algorithm solving said inverse problem and perform some calculation experiments.

Another thing we want to address here is the real life application of our model. There are several problems coming up. Firstly, our model relies on certain limitations. Right in the beginning, we assume that the thermal waves are absorbed at the surface of the top layer. This does not hold true for every material. For example, transparent top layers do not possess this property. Thus, in this case, the model does not work sufficiently.

Moreover, we assumed that the substrate layer is thermally thick, saying that there are no further reflections at the boundary since the material is assumed to be "infinitely" extended. In real life applications, we cannot restrict to that case in general, since the influence of the substrate layer results in a temperature change that has to be included.

Further, in our calculations, we chose a certain range of initial values, knowing the exact thicknesses of the layers. In real life application, one does not know that quantity. Thus, one has to make a sufficient estimation. Otherwise, there will be additional ambiguities.

Last but not least, another problem that could come up in real life applications is that in general one does not know the thermophysical properties of each material. Thus, in a first step, one has to determine these properties, leading to a more complex procedure.

Certainly, there are further problems, we are not aware of at the moment, that need to be considered.

# A   Source Code

This section contains the entire Matlab code that is used to perform the measurement experiments in Section 4. Thus, it includes the program *FullCalculation.m* where all the parameters are initialized, as well as the function *CalculatePhases.m* in blank shape without specified parameters. To be able to utilize the program code, a Matlab license is required.

**Script *FullCalculation.m*:**

```matlab
% number of layers

n = ;

% thermophysical properties of the materials M_1,...,M_n

kappa = []  ;
c = [];
rho = [];

% exact data

L_exact = ;

% excitation frequency(ies)

omega = [];

% measured phase(s)

measured_phase = CalculatePhases(L_exact,omega,n,kappa,c,rho);

% noisy measured phase(s) random

measured_phase_noisy = measured_phase + %

% initial values

L_initial_vector = [];


for k = 1:size(L_initial_vector.')

    % function that should be minimized

```

```matlab
36        fun = @(L) CalculatePhases(L,omega,n,kappa,c,rho) -
            measured_phase;
37
38        % function value at the initial value
39
40        fun_initial(1,k) = fun(L_initial_vector(1,k));
41
42        % calculated thickness(es)
43
44        L_calculated(1,k) = lsqnonlin(fun,L_initial_vector(1,k));
45
46        % function value at the result(s)/error
47
48        fun_L_calculated(1,k) = fun(L_calculated(1,k));
49
50   end
51
52   % rable of the results
53
54   T = table(L_initial_vector.',L_calculated.',(fun_L_calculated./
        measured_phase).');
55
56   T.Properties.VariableNames = {'L_initial','L_calculated','phase
        difference (omega)'};
```

**Function *CalculatePhases.m*:**

```matlab
function phase = CalculatePhases(L,omega,n,kappa,c,rho)
% L = [L_1,...,L_n-1], omega = [omega_1,...omega_m] , kappa = [
    kappa_1,...,kappa_n], c = [c_1,...,c_n], rho = [rho_1,...,
    rho_n]

% preallocation

phase = zeros(size(omega));
R = ones(1,n);
mu = zeros(1,n-1);
sigma = zeros(1,n-1);
Gamma = zeros(1,n-1);

for i = 1:length(omega)

    % reflection coefficients R_1,...,R_n-1

    for k = 1:n-1
        R(1,k+1) = (sqrt(kappa(1,k)*c(1,k)*rho(1,k))-sqrt(kappa
            (1,k+1)*c(1,k+1)*rho(1,k+1)))/(sqrt(kappa(1,k)*c(1,k)
            *rho(1,k))+sqrt(kappa(1,k+1)*c(1,k+1)*rho(1,k+1)));
    end

    % thermal diffusion length mu = [mu_1,...,mu_n-1]

    for k=1:n-1
        mu(1,k) = sqrt((2*kappa(1,k))/(rho(1,k)*omega(i)*c(1,k))
            );
    end

    % wave vectors sigma = [sigma_1,...,sigma_n-1]

    for k = 1:n-1
        sigma(1,k) = (1+1i)/mu(1,k);
    end

    % effective reflection coefficient Gamma

    Gamma(1,n-1) = R(1,n);

    for k = n-2:-1:1
        Gamma(1,k) = (R(1,k+1) + Gamma(1,k+1)*exp(-2*sigma(1,k
            +1)*L(1,k+1)))  /(1+R(1,k+1)*Gamma(1,k+1)*exp(-2*sigma
```

```matlab
                    (1,k+1)*L(1,k+1)));
        end

        % temperature T

        T = (1+Gamma(1,1)*exp(-2*sigma(1,1)*L(1,1)))/(1-R(1,1)*Gamma
            (1,1)*exp(-2*sigma(1,1)*L(1,1)));

        % phase angle(s)

        phase(i) = angle(T);

        phase(i) = rad2deg(phase(i));

    end

end
```

# References

[1] Jean Baptiste Joseph Fourier. *Théorie analytique de la chaleur*. Ulan Press, 1822.

[2] Clemente Ibarra Castanedo. *Quantitative Subsurface Defect Evaluation by Pulsed Phase Thermography: Depth Retrieval with the Phase*. Clemente Ibarra Castanedo, 2005.

[3] Francesco Ciampa, Pooya Mahmoodi, Fulvio Pinto, and Michele Meo. *Recent Advances in Active Infrared Thermography for Non-Destructive Testing of Aerospace Components*. MDPI Sensors, 2018.

[4] Alexander Dillenz, Thomas Zweschper, Gernot Riegert, and Gerd Busse. *Progress in phase angle thermography*. AIP Publishing, 2003.

[5] Yasmina Fedala, Mihaela Streza, Francisco Sepulveda, Jean Paul Roger, Gilles Tessier, and Christine Boué. *Infrared Lock-in Thermography Crack Localization on Metallic Surfaces for Industrial Diagnosis*. Journal of Nondestructive Evaluation, 2013.

[6] Thomas Lüthi. *Infrared thermography*. Materials and Structures, Vol. 31, 1998.

[7] Jin-Yu Zhang, Xiang bin Meng, and Yong chao Ma. *A new measurement method of coatings thickness based on lock-in thermography*. Elsevier, Infrared Physics & Technology 76, 2016.

[8] Dipl.-Ing. Christian Spiessberger. *Merkmalsanalyse mit thermischen Wellen in der zerstörungsfreien Werkstoff- und Bauteilprüfung*. OPUS - Online Publikationen der Universität Stuttgart, 2012.

[9] Zurich Instruments. *Principles of lock-in detection and the state of the art*. Zurich Instruments, 2016.

[10] Roger Brown. *Physical Testing of Rubber*. Springer, 2006.

[11] Deborah D.L. Chung. *Composite Materials*. Springer, 2010.

[12] Darryl Almond and Pravin Patel. *Photothermal Science and Techniques*. Chapman & Hall, 1996.

[13] John H. IV Lienhard and John H. V Lienhard. *A Heat Transfer Textbook*. Phlogiston Press, 2020.

[14] Horatio Scott Carslaw and John Conrad Jaeger. *Conduction of Heat in Solids*. Oxford University Press., 1947.

[15] Gerd Litfin. *Technische Optik in der Praxis*. Springer, 2004.

[16] Helmut Prekel, Gert Goch, and Christoph Ament. *Simulation und Anwendung photothermischer Verfahren im Labor und unter prozessnahen Bedingungen*. Universität Bremen, 2016.

[17] O Raghu and J Philip. *Thermal properties of paint coatings on different backings using a scanning photo acoustic technique.* Measurement Science and Technology, 2006.

[18] Datong Wu and Gerd Busse. *Lock-in thermography for nondestructive evaluation of materials.* Elsevier Masson SAS, 1998.

[19] Gerd Busse, Datong Wu, and Walter Karpen. *Thermal wave imaging with phase sensitive modulated thermography.* Journal of Applied Physics 71, 3962, 1992.

# List of Figures

# List of Tables